Transportation Research Interdisciplinary Perspectives 36 (2026) 101841

Contents lists available at ScienceDirect

Transportation Research Interdisciplinary Perspectives

journal homepage: www.sciencedirect.com/journal/transportation-research-interdisciplinary-perspectives

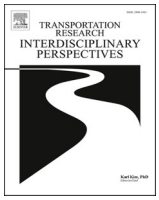

Arctic shipping under global change: A case study of offshore oil exports

Taryn Waite [c], Siwa Msangi [b,*], Ying Zhang [a], Molly French [d], Nazar Kholod [a], Jae Edmonds [a], Stephanie T. Morris [a]

[a] Joint Global Change Research Institute, Pacific Northwest National Laboratory, 5825 University Research Court, Suite 3500, College Park, MD 20740, USA
[b] International Institute for Applied Systems Analysis, Schlossplatz, A-2361 Laxenburg, Austria
[c] Minnesota Department of Commerce, 85 7th Place East, Suite 280, Saint Paul, MN 55101, USA
[d] Oakton College, 1600 Golf Rd, Des Plaines, IL 60016, USA

ARTICLE INFO

Keywords:
Northern Sea Route
Arctic
Shipping
Sea ice
Offshore oil

ABSTRACT

We explore impacts of sea ice thinning and evolutions in the energy sector on future use of the Northern Sea Route (NSR) versus the Suez Canal Route (SCR), using a case study of shipping oil extracted from the offshore Russian Arctic to China. We combine an integrated human-Earth system model with a shipping cost model to incorporate impacts on both oil production and shipping costs under internally consistent scenarios. We find that the NSR could become cost-competitive with the SCR as sea ice thickness declines, especially in an RCP8.5 scenario, due to decreasing fuel and icebreaker escort costs. In a global energy evolution scenario consistent with RCP2.6, high emissions costs on the longer SCR may outweigh the costs associated with thicker sea ice on the NSR. Our novel framework provides integrated projections of NSR shipping traffic and associated emissions driven by potential Arctic offshore oil production and exports.

1. Introduction

The continuing pace of warming in the Arctic has been driving the decline of sea ice extent and thickness over the past decades and this trend has been accelerating in recent times (Lasserre, 2014), increasing shipping accessibility in the region. Arctic shipping traffic is already growing, with a 43% increase in the number of unique ships recorded within the Arctic and a more than doubling of total distance traveled from 2013 to 2023 (Arctic Council, 2024). While much of the current shipping activity in the Arctic Polar Code Area is local traffic such as fishing vessels (Arctic Council, 2024), sea ice decline and advancements in icebreakers are increasing possibilities for *trans*-Arctic commercial shipping, particularly through the Northern Sea Route (NSR). Trans-Arctic shipping introduces the potential for significant time and cost savings in transit compared to conventional Southern routes connecting Europe and Asia (Aksenov et al., 2017). 2024 was a record year for NSR transit shipments, with a total of 97 transit voyages carrying over 3 million tons of cargo combined (Centre for High North Logistics, 2024).

Research has shown that the commercial viability of the NSR is projected to improve, in terms of both navigable season length (Chen et al., 2020; Khon et al., 2017) and the possible shipping speeds along the route, allowing for shorter transit times (Melia et al., 2016). However, the extent of potential future NSR traffic will depend on not only sea ice conditions, but also the characteristics of and demand for specific goods that could be shipped. The use of the NSR for high-value commercial shipping has been problematic and limited in the past due to concerns over volatile weather conditions, complex geography, sparse logistical and safety infrastructure, and geopolitical considerations (Wan et al., 2021). While these factors have prevented large-scale shipping on the NSR to date, conventional routes like the Suez Canal Route (SCR) have their own substantial risks such as exposure to cyclones and piracy; the NSR in fact may have the long-term potential to become a less risky alternative to the SCR (Christensen et al., 2019). Further, given that the NSR is substantially shorter than its alternatives and thus offers CO_2 emissions reductions potential, it could become increasingly competitive under scenarios of global change consistent with low-emission futures (Cariou & Faury, 2015).

In this analysis, we evaluate the economic feasibility of shipping oil extracted from the offshore Russian Arctic to China. Growing natural resource extraction activities are a prominent driver of increasing Arctic shipping demand (Arctic Council, 2024). In particular, shipments of oil from Russia to China comprised 65% of all cargo transported via transit

* Corresponding author.
E-mail addresses: msangi@iiasa.ac.at (S. Msangi), ying.zhang@pnnl.gov (Y. Zhang), mollyfrench4@outlook.com (M. French), nazar.kholod@pnnl.gov (N. Kholod), jae@pnnl.gov (J. Edmonds), stephanie.morris@pnnl.gov (S.T. Morris).

https://doi.org/10.1016/j.trip.2026.101841
Received 8 April 2025; Received in revised form 3 January 2026; Accepted 5 January 2026
Available online 19 January 2026

shipments on the NSR in 2024 (Centre for High North Logistics, 2024). Further, the sea ice decline responsible for opening the NSR will also increase accessibility of Arctic offshore oil resources (Petrick et al., 2017). At the same time, potential evolutions toward global low emissions economies could have implications for future global fossil resource demand (Bauer et al., 2015; Lazarus and van Asselt, 2018). Thus, this presents an opportunity to holistically assess changes in shipping patterns and volumes driven by thinning Arctic sea ice and changing global energy markets on the demand, production, and transportation of a globally important commodity likely to be shipped on the NSR.

We integrate these factors by combining sea ice thickness projections from General Circulation Models (GCMs) with projections of socioeconomic variables from the Global Change Analysis Model (GCAM), an integrated human-Earth system model (Calvin et al., 2019). Previous research has used GCAM to project future Russian Arctic offshore oil production under different scenarios of global change, including sea-ice thinning and changing global energy demand (Zhang et al., 2024). These scenarios incorporate the impacts of future changes to sea ice thickness on the cost of oil extraction, as well as the impacts of global low emissions scenarios on global oil demand and (shipping) fuel prices. These dynamics can inform shipping fuel costs, including emissions costs consistent with different Representative Concentration Pathways (RCPs). We pair the GCAM oil production, shipping fuel prices, and emissions cost projections from Zhang et al.'s (2024) study with a shipping model; this allows us to compare the feasibility of shipping the oil produced in the offshore Russian Arctic to East Asia over the NSR versus the SCR in different scenarios of future Arctic sea ice thinning and global energy system evolutions. We then explore the potential implications for NSR shipping traffic and associated CO_2 emissions. Our approach provides us with an interdisciplinary perspective on how the economics of shipping are affected by changing conditions in the Arctic, as captured by physical earth systems models; and how those interact dynamically with the energy sector and other key components of human systems embodied within GCAM. The approach for linking GCAM with our analysis will be explained further in the methodology section.

In the literature review, we highlight key components of existing NSR cost analyses and identify gaps in the literature. In the methods section, we describe the overall framework including our shipping model. We present our results in terms of changes in NSR navigability, potential shipping volumes and traffic along the NSR given the cost differences between routes, and associated CO_2 emissions from shipping. Based on these results, we highlight our key findings and summarize the implications for further research in this area.

2. Literature review

Historical datasets show a substantial decline in Arctic sea ice thickness and extent over the past several decades (Kwok, 2018; Box et al., 2019). GCMs project continued sea ice decline, with most projecting a September sea ice-free Arctic Ocean for the first time by 2050 (Notz et al., 2020). Several studies have assessed the implications for future *trans*-Arctic shipping potential in terms of increasing season length (Oh et al., 2017; J. Chen et al., 2020; J. Chen et al., 2021; S. Chen et al., 2022), increasing navigable area (Stephenson et al., 2011), and decreasing transit times along *trans*-Arctic routes (Melia et al., 2016; Askenov et al., 2017).

The extent to which the NSR and other *trans*-Arctic shipping routes will be used depends on their economic competitiveness with non-Arctic alternatives. Numerous studies have modeled the cost of shipping on Arctic routes compared to non-Arctic routes, focusing on both the current situation (Cariou and Faury, 2015; Faury and Cariou, 2016; Cheaitou et al., 2022; Faury et al., 2020; Lasserre, 2014; Meza et al., 2023; Sibul and Jin, 2021; Theocharis et al., 2019, 2022; Wang et al., 2020; Zhang et al., 2016; Pruyn and van Hassel, 2022) and potential future conditions (Aksenov et al., 2017; Christensen et al., 2019; Gleb and Jin, 2021; Khon et al., 2017; Li et al., 2023; Melia et al., 2016; Wang et al., 2023). Key inputs to these cost models include sea ice conditions, bunker fuel costs, ice breaker escort fees, operating and vessel capital costs, and potential policies and regulations.

Sea ice conditions are an important driver of current and future NSR costs since they can impact vessel speed as well as the need for icebreaker escorts. However, treatment of sea ice conditions within NSR cost models ranges in complexity. Some studies do not explicitly model sea ice thickness or extent and instead assume a slower average speed when traveling on the NSR compared to on open water (Theocharis et al., 2019, Zhang et al., 2016; Theocharis, 2024). Others use historical sea ice thickness (SIT) data to estimate current SIT along the NSR or to define bounds and sensitivity cases (Wang et al., 2020; Faury and Cariou, 2016; Cheaitou et al., 2022; Gleb and Jin, 2021). Some studies use projections of SIT to evaluate NSR transit costs in future periods (Faury et al., 2020; Wang et al., 2020).

For studies that explicitly model SIT, a well-established approach uses SIT thresholds to determine conditions in which a vessel (a) can navigate freely at its design speed, (b) can navigate freely at a slowed speed, (c) can only navigate when accompanied by an ice breaker escort, or (d) cannot navigate at all. Slowed speeds are usually calculated as a function of SIT based on a negative exponential relationship (Faury and Cariou, 2016; Faury et al., 2020; Wang et al., 2020; Gleb and Jin, 2021). Cheaitou et al. (2022) used a similar approach, but calculated navigability thresholds and reduced speeds based on the POLARIS Risk Index Outcome, an indicator derived from SIT. Given the sailing speeds determined by these sea ice thresholds, daily fuel consumption is often calculated based on a cubic function that depends on the sailing speed, the vessel's design speed, and fuel consumption efficiency (Wang and Meng, 2012). Studies estimate vessel speed in the absence of sea ice either by assuming that the design speed will be maintained (Cheaitou et al., 2022; Faury et al., 2020) or by estimating optimal speeds to maximize profits or minimize shipping costs (Theocharis et al., 2019; Theocharis et al., 2024).

Bunker fuel prices, applied to total fuel consumption in shipping cost models, are an important determinant of NSR competitiveness since fuel can make up a large proportion of total voyage costs (Li et al., 2023). Thus, most studies conduct sensitivity analyses on fuel price based on either historical price fluctuations or proportional changes from current prices (Theocharis et al., 2019; Wang et al., 2020; Zhang et al., 2016; Theocharis, 2014; Faury et al., 2020; Gleb and Jin, 2021).

Theocharis et al. (2019) and Wang et al. (2020) both showed that icebreaker escort fees, and their associated uncertainty, can be a crucial factor in determining NSR competitiveness. Most studies adopt baseline fees following the official Northern Sea Route Administration (NSRA) guidelines released in 2014, which dictate fees depending on season, vessel ice class, gross tonnage, and number of NSR zones in which an escort is needed (Theocharis et al., 2019; Wang et al., 2020; Cheaitou et al., 2022; Theocharis, 2024; Faury et al., 2020; Faury and Cariou, 2016; Gleb and Jin, 2021). Some studies use SIT data to calculate these fees based on the number of zones needing an escort (Faury and Cariou, 2016; Gleb and Jin, 2021). Others make the simplifying assumption that an escort will be needed in all zones in a baseline scenario and analyze additional sensitivities assuming independent navigation or the need for an escort in some but not all zones (Wang et al., 2020; Theocharis et al., 2019; Theocharis, 2024).

Since the official NSRA escort fees are provided in Russian rubles (RUS), NSR shipping costs in U.S. dollars (USD) depend on the RUB/USD exchange rate which can fluctuate significantly (Shibasaki et al., 2018). Thus, some studies conduct sensitivity analyses of NSR costs using different exchange rates (Theocharis et al., 2019; Theocharis et al., 2024; Gleb and Jin, 2021). Given that the RUB/USD exchange rate strongly correlates with bunker fuel price (Shibasaki et al., 2018), studies tend to pair exchange rate sensitivities with fuel price sensitivities according to this relationship (Theocharis et al., 2019; Theocharis et al., 2024; Gleb and Jin, 2021). Moreover, since the official NSRA guidelines dictate the upper limit on fees that can be charged, the

possible use of discounted fees introduces additional uncertainty; some studies have thus considered scenarios with discounted rates based on historical evidence (Theocharis et al., 2019, Wang et al., 2020; Theocharis, 2024).

Most analyses estimate daily operations costs and apply them to the duration of a voyage, which depends on speed along the route (Faury and Cariou, 2016; Faury et al., 2020; Cheaitou et al., 2022; Theocharis et al., 2024). Some studies consider individual components of operating costs such as wages, repair, and insurance premiums (Li et al., 2023; Gleb and Jin, 2021) – with some also taking the hinterland transport processes into account, so they can compare maritime (NSR or non-NSR) routes with overland transportation, under current conditions (Pruyn and van Hassel, 2022). Many also incorporate capital costs of vessels (Theocharis et al., 2019; Wang et al., 2020; Zhang et al., 2016; Cheaitou et al., 2022; Theocharis et al., 2024; Gleb and Jin, 2021); however, some exclude capital costs under the assumption that the vessels are already in operation and capital costs will not differ with route choice (Li et al., 2023; Faury et al., 2020; Faury and Cariou, 2016).

A few studies have incorporated environmental regulations related to ships' fuel types, greenhouse gas emissions, and pollutant emissions into their cost models. Theocharis et al. (2019) assessed the impact of efforts to promote less polluting fuels, including a global fuel tax and a heavy fuel oil (HFO) ban, on NSR competitiveness. Wang et al. (2020) and Cheaitou et al. (2022) both incorporated CO2 taxes on shipping emissions into their cost model.

Studies assessing long-term future NSR cost competitiveness tend to only explicitly project SIT, with the key economic factors described above included as sensitivity cases rather than dynamic, integrated projections that include evolving socioeconomic conditions. To our knowledge, no NSR studies have used integrated human-Earth system models to analyze scenarios of socioeconomic factors and consistent projected sea ice conditions. Our approach adds to the literature by modeling future NSR cost competitiveness based not only on projected SIT, but also on the following key socioeconomic variables that are informed by an integrated human-Earth system model (GCAM):

1. Quantity produced of the commodity that needs to be shipped (i.e., demand for shipments);
2. Shipping fuel prices;
3. Emissions costs associated with the evolution of a global low-emission energy system.

3. Methodology

In this section, we present our overall analytical framework (Section 3.1), and describe the case study that we apply it to (Section 3.2). Given the importance of results from Zhang et al.'s (2024) GCAM analysis to our framework, we give details on these results in Section 3.3. The subsequent sections describe our model of shipping cost and route choice (Sections 3.4-3.6).

3.1. Overall framework

In our paper we bring together Zhang et al.'s (2024) projections of

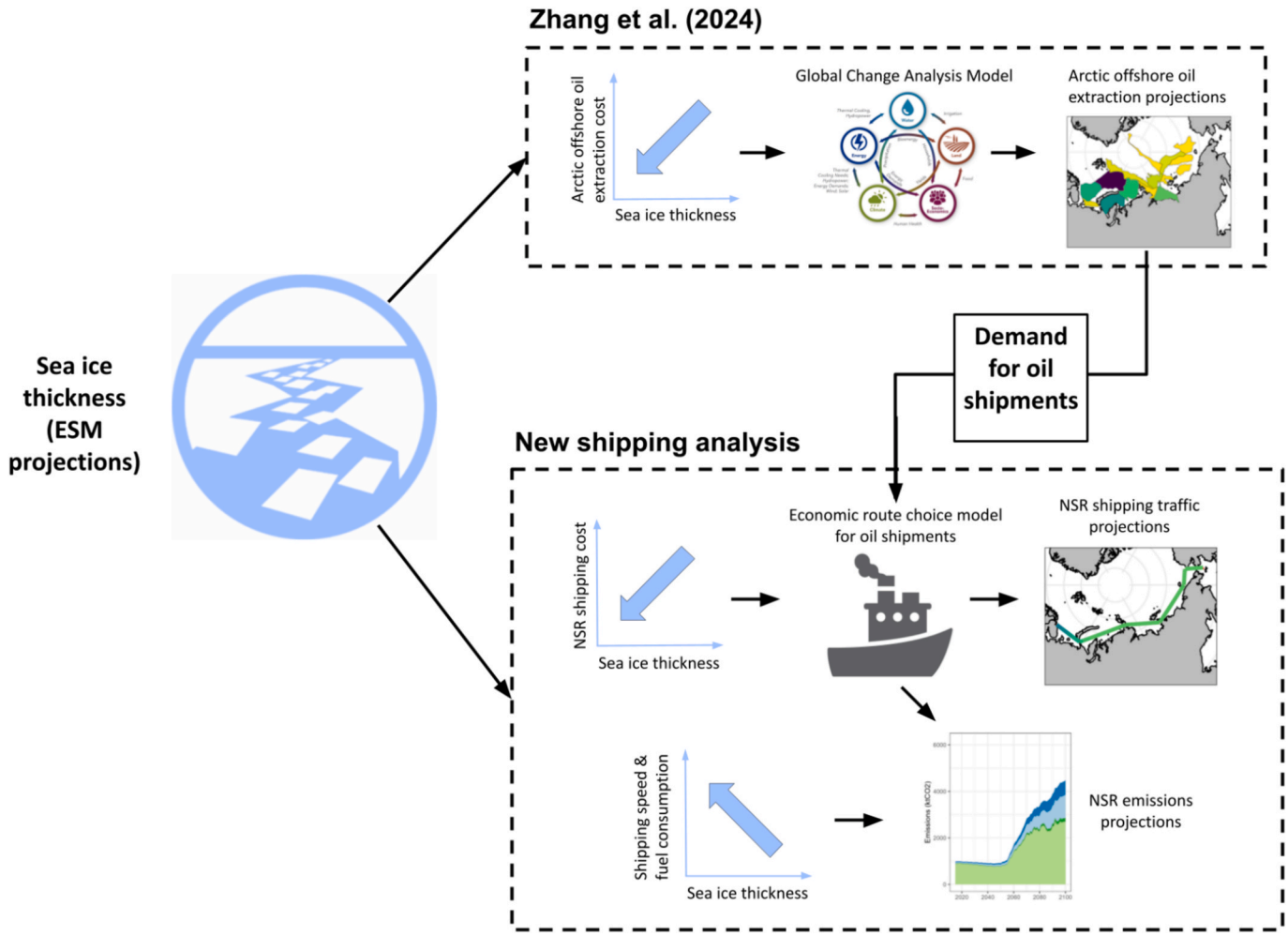

Fig. 1. Linkages between CMIP6 sea ice thickness projections, Zhang et al.'s (2024) GCAM analysis, and our new shipping analysis.

Arctic offshore crude oil from GCAM with an analysis of shipping potential through the NSR. Both components are impacted by SIT in the Arctic, which is projected by the Earth Systems models (ESMs) used in Phase 6 of the Coupled Model Intercomparison Project (CMIP6). We use SIT projections consistent with those used by Zhang et al. (2024)'s study to drive our simulations of shipping traffic through the NSR. Fig. 1 illustrates how projected changes in SIT from the ESMs affect projected Arctic offshore oil extraction in Zhang et al.'s (2024) analysis as well as projected costs of NSR shipping, shipping speeds, and fuel consumption in our new shipping analysis. See Sections 3.3 To 3.6 for more details on these dynamics. Fig. 1 also illustrates how we incorporate Zhang et al.'s (2024) results into our analysis by inferring demand for oil shipments from the GCAM oil extraction projections and using this demand to set the scale for our economic route choice model. In Zhang et al.'s (2024) analysis, declining SIT lowers offshore extraction costs and increases Arctic offshore oil production. In our shipping analysis, the same SIT trajectories reduce NSR shipping costs and allow higher sailing speeds, influencing route choice, fuel use, and emissions.

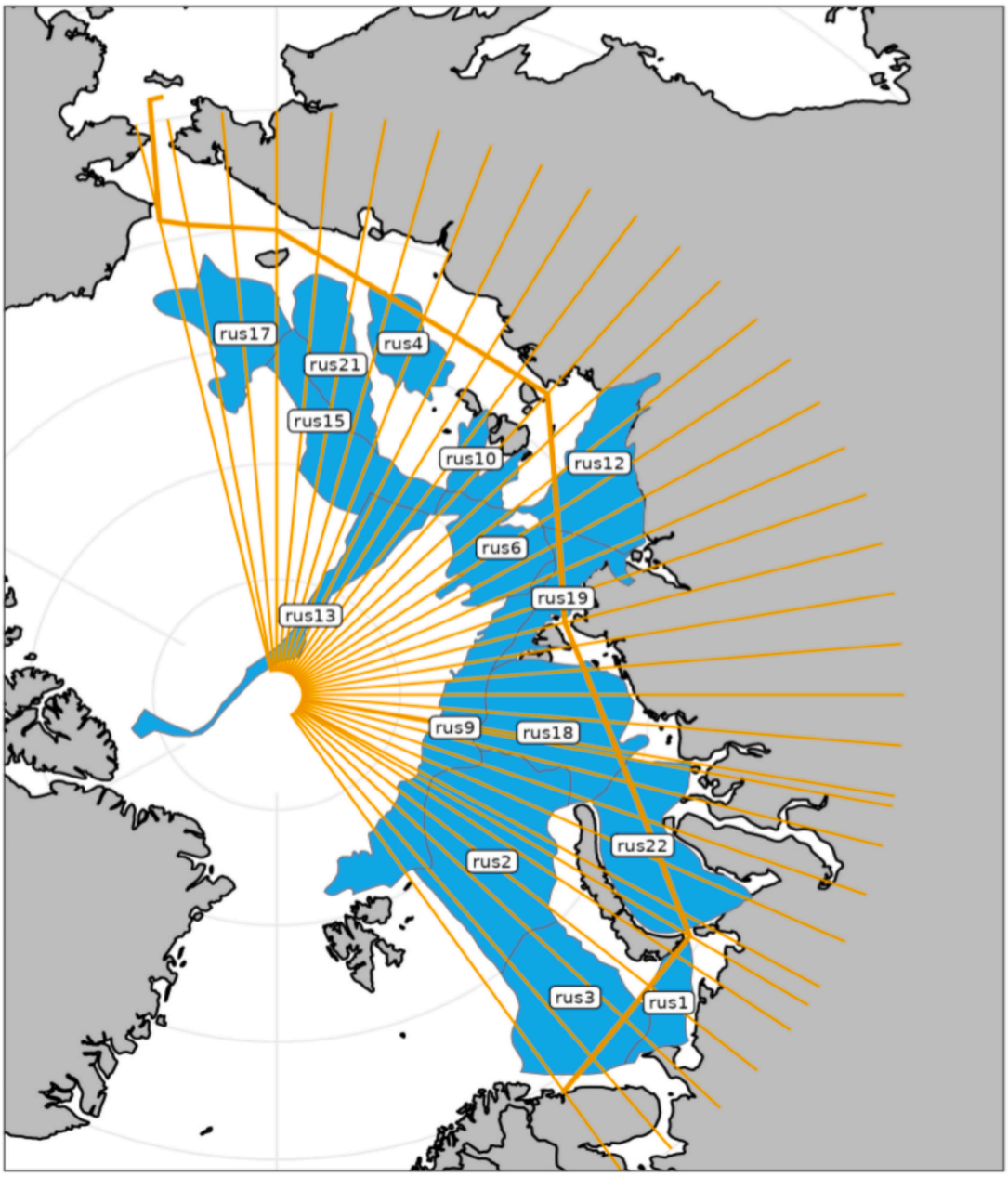

rus1: Kolguyev Terrace	rus2: North Barents Basin	rus3: South Barents Basin and Ludlov Saddle
rus4: East Siberian Sea Basin	rus6: Lena Prodelta	rus9: Nansen Basin Margin
rus10: Anisin-Novosibirsk Basins	rus12: West Laptev Grabens	rus13: Makarov Basin Margin
rus15: Siberian Passive Margin	rus17: North Chukchi-Wrangel Foreland	rus18: North Kara Basins and Platforms
rus21: Vilkitskii Basin	rus22: South Kara Sea Offshore	

Fig. 2. Map of the study region. USGS Assessment Units (AUs) for offshore oil resources are shown in blue, the Northern Sea Route (NSR) is shown in bold orange. The light orange lines show the longitudinal boundaries of the 36 NSR subzones defined by Cheaitou et al. (2019).

3.2. Case study description

We apply the framework described above to the case study of shipping oil produced in the offshore Russian Arctic to the port of Dongjiakou, China. These offshore oil resources are located along the Russian Arctic coast, and are located in United States Geological Survey (USGS)-defined "Assessment Units" (AUs), as is shown in Fig. 2.

Dongjiakou serves as a useful point of reference given its location within a fast-growing, northern region of China (Shandong) and recent efforts to greatly expand its oil storage capacity (Shandong Port Group Co., Ltd., 2023). The fact that many of the current ports that import crude oil into China are located in the vicinity of Donjiakou (Si, 2021), further justifies this as our representative destination point for the oil shipments that go along the NSR.

For three scenarios considering different future sea ice and global energy system conditions (Table 1), we compare projected navigability and costs of shipping oil along two routes: (1) eastward along the NSR, through the Bering Strait, and down the East Asian coast (hereafter referred to as the East route); and (2) westward along the NSR, through the Baltic region, around the West of Europe, and through the Suez Canal Route to Asia (hereafter referred to as the West route). The definition of the NSR that we use for our shipping calculations is consistent with Cheaitou et al (2019), which extends from the ports of Murmask, Russia on the western end, to that of the Bering Strait on the eastern end (Fig. 2). The additional distance between the Bering Strait and Dongjiakou is accounted for in our analysis. For our shipping analysis, we segment the NSR into 36 subzones as defined by Cheaitou et al. (2019). This spatial resolution allows us to consider varying SIT conditions along the NSR and also allows us to model oil shipments originating at 36 different points along the NSR. The longitudinal boundaries of the subzones, and where these boundaries intersect with the oil AUs, is shown in Fig. 2. See Section 3.5 for more details on how we determine the starting points of oil shipments in our model. Note that, as most oil is expected to be extracted from regions near the western end of the NSR (Zhang et al., 2024), the East route traverses a substantially longer portion of the NSR than the West route for most shipments.

The first two scenarios, *BAU|8.5* and *BAU|2.6*, combine a business-as-usual global energy system evolution with sea ice projections based on two different representative concentration pathways (*RCP2.6* and *RCP8.5,* respectively). The RCPs are a set of global scenarios developed by the research community to encompass a range of possible radiative forcing outcomes for the century (van Vuuren et al., 2011). RCP2.6 describes a relatively low greenhouse gas (GHG) emissions scenario in which radiative forcing reaches 2.6 W/m^2 by the end of the century, whereas RCP8.5 represents a scenario reaching 8.5 W/m^2. The third scenario, *LowC|2.6*, considers sea ice change consistent with RCP2.6 and a global energy system evolution resulting in a GHG emissions trajectory consistent with RCP2.6, a relatively low carbon emission trajectory compared to the business-as-usual case.

We compare projected navigability and costs along the two routes under these scenarios for two different vessel types, ice class 1A and ice class 1AS, which are among the most frequently-used ice class vessels for the NSR (Erikstad & Ehlers, 2012 as cited in Faury & Cariou, 2016). Among the Finnish-Swedish ice class definitions, 1AS and 1A are the highest- and second highest-strength vessel types, respectively (Riska and Kämäräinen, 2011) and correspond roughly to the Russian Arc4 and Arc5 ice classes (HELCOM, 2016). There are vessels with higher standards of ice-strengthening and operational capabilities that can convey oil and gas, such as the PC3/Arc7 vessels. While some of these have been observed in use on the NSR in recent years (Staalesen, 2024), we chose to focus on the 1A and 1AS vessels in this analysis due to more readily available technical parameters that characterize their speed and fuel consumption across varying SIT conditions. Given the navigability and costs to ship along the two routes, we use an economic choice model to project, for each scenario, the quantities of oil shipped over each route on a monthly basis through 2100. Fig. 3 provides an overview of this route choice framework with detailed descriptions in the following sections.

Table 1
Description of scenarios.

Scenario name	Global energy system evolution	Sea ice thickness
BAU|8.5	Business-as-usual	RCP8.5
BAU|2.6	Business-as-usual	RCP2.6
LowC|2.6	Consistent with RCP 2.6	RCP2.6

3.3. Projected oil production

We use Zhang et al.'s (2024) projections of offshore oil production from 15 AUs in the Russian Arctic under the three scenarios described above. These projections were produced using the Global Change Analysis Model (GCAM v5.3), a global, integrated human-Earth system model that links the energy, socioeconomic, land, water, and climate systems and simulates their interaction and evolution under alternative socioeconomic and environmental pathways. Zhang et al. (2024) modeled Arctic offshore oil production in GCAM by developing functions to estimate the extraction costs that would be incurred if oil and gas potentials in the AUs were exploited under projected sea-ice conditions in the future. Thinner projected sea ice corresponds with lower extraction costs. Combined with Arctic offshore resource potential in each AU estimated by USGS, these costs define the offshore Arctic hydrocarbon resource supply curves over time given different sea-ice conditions under different RCPs. The model resolves both regional supply–demand equilibrium and global trade balances (imports and exports) through competitive markets in which prices are solved endogenously. The model is calibrated to the historical Arctic offshore oil and gas production in line with known reserves and resource supply curves. Consistent with the scenarios in this study, the *LowC|2.6* scenario in Zhang et al. (2024) reflects changing supply, demand, price, and trade of energy resources as the global energy system evolves to achieve an emissions pathway consistent with RCP2.6. Note that both *BAU|2.6* and *LowC|2.6* use the same sea ice projections; however, *LowC|2.6* further incorporates incentives for societal and technological changes (e.g., higher electrification) that drives energy system evolution, achieving the intended low carbon emission trajectory.

Zhang et al.'s (2024) total oil extraction projections in these scenarios from the 15 Russian Arctic AUs are shown in Fig. 4. Russian Arctic oil production increases throughout the century in all scenarios (Zhang et al., 2024), reaching the highest quantity in 2100 under the *BAU|8.5* scenario (Fig. 4). Greater ice thickness and resulting higher costs of extraction hinders the growth of oil production under the *BAU|2.6* scenario. However, in the *LowC|2.6* scenario, which incorporates the low-carbon economic incentives through carbon tax (and global economy-wide adjustments) necessary to achieve the carbon mitigation targets of the RCP 2.6 pathways, there is an additional increase in crude oil extraction in the Arctic, compared to the reference RCP2.6 case (i.e., BAU|2.6). This is because Arctic offshore oil is relatively clean and can replace the higher-emissions unconventional oil production to meet the overall oil demand. This effect largely offsets this ice thickness effect and brings Russian Arctic oil production up to levels comparable to the *BAU|8.5* scenario by 2100. In the variant RCP 2.6 scenario (i.e., LowC|2.6).

Furthermore, the extraction of offshore crude oil begins earlier in the projections horizon under BAU|8.5, compared to the BAU|2.6 case. Fig. S1 shows the spatial distribution of the oil extraction across the AUs and Table 2 shows the starting dates of oil production in each AU across scenarios, as simulated by GCAM. Table 2 and Fig. S2 both show the pattern of oil extraction beginning first at the "edges" of the Arctic region, with the AUs closer to the middle becoming accessible later in time.

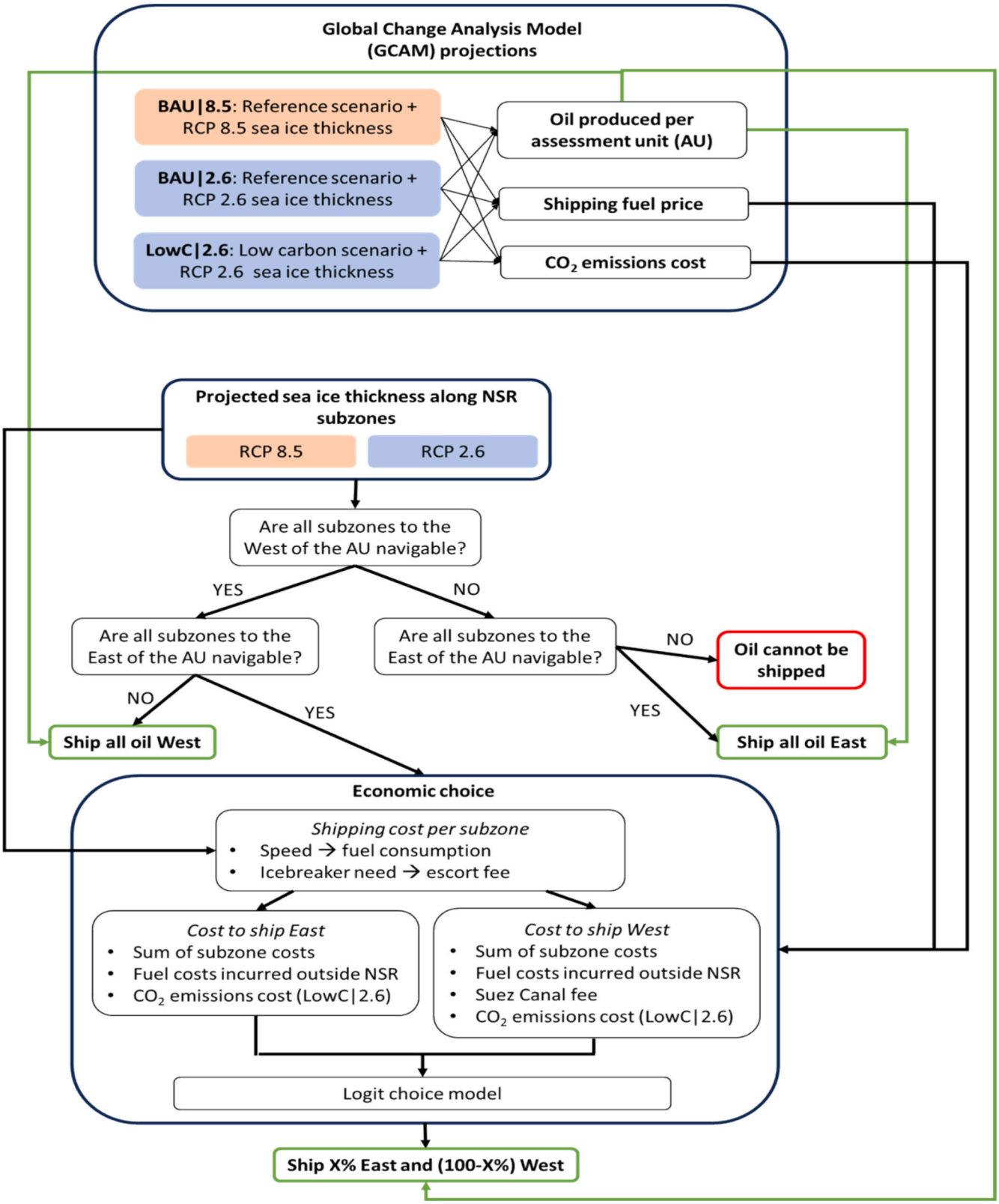

Fig. 3. Overview of methodology to project the quantity of oil shipped over each route.

3.4. NSR navigability and speed

As introduced in Section 3.2, following the approach of Cheaitou et al. (2019), we partition the NSR into 36 subzones, starting from the port of Murmansk and ending at the Bering Strait. These subzones are subsections within the 7 zones defined by the Northern Sea Route Administration. The subzones provide a finer spatial resolution, allowing us to capture variation in sea ice conditions along the NSR. We assume that oil produced in a given AU can either be shipped eastward on the NSR toward the Bering strait (following the East route) or westward

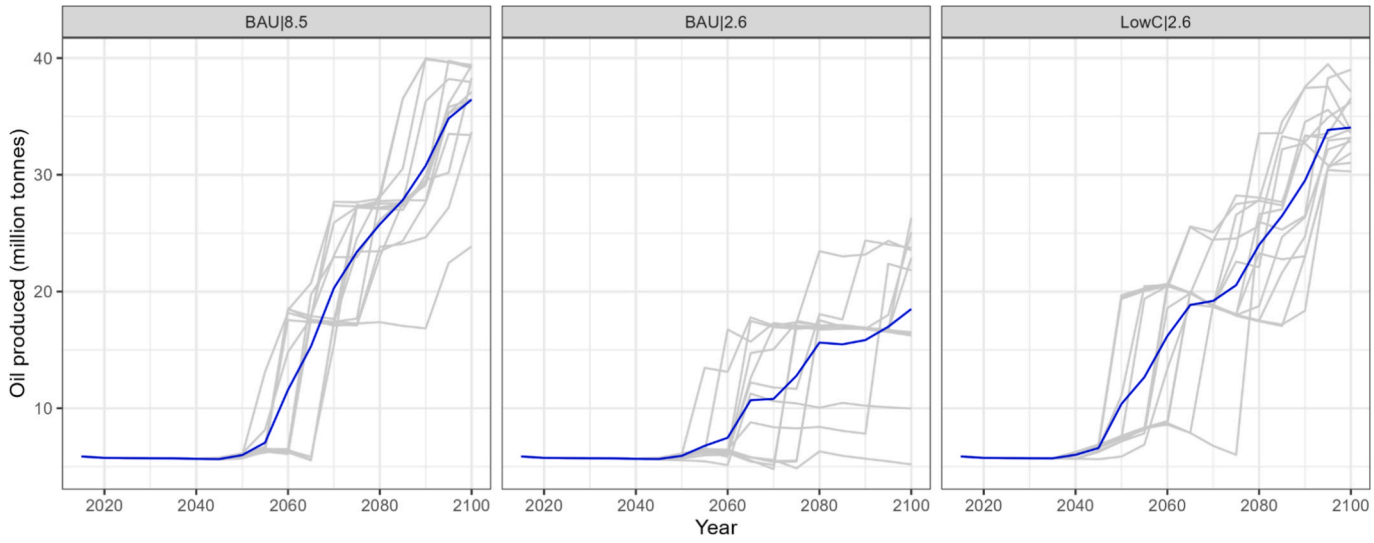

Fig. 4. Projected total extraction of crude oil from the Russian Arctic offshore region under the BAU|8.5, BAU|2.6, and LowC|2.6 scenarios from GCAM, based on results from Zhang et al. (2024). All ensembles are shown in grey and the ensemble average is shown in blue.

on the NSR toward Murmansk and the SCR (following the West route). Note that we assume the ships follow an NSR route parallel to the coastline and that we do not dynamically plot feasible routes on a grid cell by grid cell basis as sea-ice thickness changes. This type of dynamic programming approach can be used to determine alternative least-cost routes which may include shorter routes that pass nearer to the Arctic circle (Melia et al., 2016). However, this approach is beyond the scope of our analysis; our simplified approach relies on the fixed shipping distances along the NSR consistent with Cheaitou et al (2019).

To determine the navigability and relative costs of the East and West routes, we first assess which NSR subzones a vessel would need to traverse on an East or West trip carrying an oil shipment from a given AU. We determine the NSR subzone from which the oil shipment would start its trip based on the relative longitudes of the AU and the NSR subzones (Figs. 2 and S2). Since some AUs span more than one subzone, we split each AU into multiple "subAUs," corresponding to each subzone with which the AU overlaps in terms of longitude. We then partition the AUs' projected oil production into these subAUs according to the proportion of the AU's longitudinal range overlapping with the corresponding subzone's longitudinal range. Note that we do not consider the additional navigation that may be needed between a potential oil extraction site and the NSR; instead, we make the simplifying assumption that shipments will begin on a subzone of the NSR that overlaps longitudinally with the AU. This allows us to derive general insights given that the AUs represent potential future regions for resource extraction, and actual locations of extraction sites and infrastructure are unknown.

We use gridded sea ice thickness projections from CMIP6 to assess monthly average sea ice thickness along the 36 subzones through 2100 under RCP 8.5 and RCP 2.6. Given the diversity in the representation of Earth systems processes and biophysical dynamics, as well as the inherent uncertainties in the trajectories of future drivers, CMIP6 contains a suite of ensemble combinations across various models that show plausible trajectories of sea ice thickness. We use the same 13 ensemble members used in Zhang et al.'s (2024) oil production projections.

We apply a set of sea ice thickness thresholds related to shipping navigability and speed for 1A and 1AS vessels to derive speed as a function of sea ice thickness (Fig. 5).

When sea ice thickness in a given subzone exceeds the vessel's navigability threshold (IT_v^n), we assume that the vessel cannot cross the subzone. This corresponds to the horizontal red line at the very bottom right of each panel in Fig. 5. Navigability thresholds are based on Faury et al. (2020). Rather than adopting their seasonally differentiated thresholds, we use the average of the summer/autumn and winter/spring thresholds year-round due to the uncertainty around whether Russian authorities will maintain seasonally differentiated NSR navigation constraints in the future (Humpert, 2018). When SIT is below the navigability threshold but above the ice breaker threshold (IT_v^b), we assume that an ice breaker escort is needed and the vessel's speed is reduced to the maximum speed of the ice breaker (3 knots). This corresponds to the orange horizontal lines in Fig. 5. When SIT is below the ice breaker threshold (i.e., an ice breaker escort is not needed) but above the speed reduction threshold (IT_v^c), the vessel's speed is reduced from its maximum speed according to Equation 1 (Faury and Cariou, 2016), where $S_{r,m,y,z,v}$ is the maximum vessel speed under RCP r in month m of year y in subzone z for vessel v (knots), i_v is the vessel's intercept parameter (Table S1), $T_{r,m,y,z}$ is the sea ice thickness (cm), and x_v is the vessel's exponent parameter. The speed reduction equation results in speeds between the maximum vessel speed (i.e., design speed, D_v) and the minimum speed before ice breaker assistance (M_v) (Equation 1). This corresponds to the sloped light green line in each panel of Fig. 5. See SI section 1.3 for an explanation of how we derived the speed reduction equation parameters, as well as for the specific values of key thresholds described here (Table S1). Below the speed reduction threshold, we assume that the vessel can operate at its maximum speed (D_v) – which corresponds to the horizontal dark green line at the top left of each panel in Fig. 5.

$$S_{r,m,y,z,v} = i_v * \left(\frac{T_{r,m,y,z}}{100}\right)^{x_v} \quad [1]$$

3.5. Transit costs

Next, we estimate the total cost of each offshore oil shipment (C_{total}) from a given subAU on the East and West routes (equation 2). Note that there are 36 potential departure points along the NSR, corresponding with the 36 subzones, from which we can calculate the shipping costs.

$$C_{total} = \left(\sum\nolimits_{z \in Z} C_{f,z}\right) + C_{f,o} + C_{IB} + C_O + C_{SC} + C_E \quad [2]$$

The total cost includes (1) the cost of fuel consumed both within each subzone z of the NSR traversed ($C_{f,z}$), where, depending on the departure point, the set of subzones traversed Z varies; (2) the cost of fuel consumed outside the NSR ($C_{f,o}$); (3) the cost of an ice breaker escort on the NSR(C_{IB}) when the monthly sea ice thickness projection exceeds the ice breaker SIT threshold; (4) the cost of operations along the whole

Table 2
Projected starting years of crude oil extraction under each scenario from GCAM – production levels averaged across CMIP6 ensembles in 5-year time-steps.

	rus1	rus2	rus3	rus4	rus6	rus9	rus10	rus12	rus13	rus15	rus17	rus18	rus19	rus21	rus22
	Kolguyev	*North Barents*	*South Barents & Ludlov*	*East Siberian Sea*	*Lena Prodelta*	*Nansen*	*Anisin-Novosibirsk*	*West Laptev*	*Makarov*	*Siberian*	*North Chukchi-Wrangel*	*North Kara*	*Northwest Laptev*	*Vilkitskii*	*South Kara*
BAU|8.5	*2020*	*2055*	*2045*	*2090*	*2085*	*2065*	*2090*	*2085*	*2090*	*2090*	*2080*	*2065*	*2075*	*2080*	*2065*
BAU|2.6	*2020*	*2055*	*2045*			*2080*						*2080*			*2080*
LowC|2.6	*2020*	*2050*	*2040*	*2090*	*2085*	*2070*	*2090*	*2080*	*2095*	*2090*	*2090*	*2070*	*2080*	*2090*	*2065*

Source: authors compilation of results from Zhang et al (2024).

transit (C_O); (5) the Suez Canal fee (C_{SC}) in the case of the West route; and (6) the emissions cost (C_E) in the case of the *LowC|2.6* scenario. Note that these emissions costs do not include the pricing framework introduced during the 83rd meeting of the Marine Environmental Protection Committee (MEPC), but are derived from the carbon prices calculated by GCAM to produce a scenario with global GHG emissions in line with RCP 2.6 (Table S2).

Fig. 6 summarizes the average costs per shipment across scenarios for the East and West routes, including the average cost per shipment (A) in total and (B) broken down into its components (as in Equation 2) including fuel costs, operation costs, ice breaker escort costs, the Suez canal fee, and emissions costs. Since costs vary depending on the starting subzone of the shipment, in the figure costs to ship from each subzone are weighted by the proportion of total oil produced in each subAU in a given month; costs are then averaged over each month in a given season (summer/ autumn and winter/ spring). All cost components except $C_{f,o}$ and C_{SC} vary with projected monthly sea ice thickness along the NSR. Aggregating the average costs by season in Fig. 6 demonstrates this variation; note that monthly sea ice thickness during the summer/ autumn season (July through November) is lower on average than monthly sea ice thickness during the winter/ spring season (December through June).

Along the NSR, we estimate fuel consumption (tons) within a given subzone as a function of vessel speed using Equation 3 (Wang and Meng, 2012, as applied by Faury and Cariou, 2016), where l_z is the length of subzone z (nautical miles or NM), $S_{r,m,y,z,t}$ is the speed of the vessel given by Equation 1 (NM/hr or knots), multiplied by 24 hr/day to convert it to NM/day, F_v is the daily fuel consumption by vessel type v at its design speed (tons/day), and D_v is the vessel's design speed (knots):

$$F_{r,m,y,z,v} = \frac{l_z}{24 * S_{r,m,y,z,v}} * \left[F_v * \left(\frac{S_{r,m,y,z,v}}{D_v} \right)^3 \right] \quad [3]$$

We calculate the total fuel consumed outside the NSR by ship type based on the distances traveled outside the NSR to reach the port of Dongjiakou which are 3,509 NM and 14,269 NM on the East and West routes, respectively (sea-distances.org), assuming that vessels can operate at their design speed while outside of the NSR as sea ice is not present. We use crude oil prices from GCAM (Table S2) as a proxy for bunker fuel price, since the two are closely correlated (Chen et al., 2022).

We calculate ice breaker escort fees based on the tariff levels published by the Russian government (Ministry of Justice of Russia, 2014). The tariffs depend on season, gross tonnage, and the number of NSR zones in which the escort is needed (Table S3). Since each of these zones contain multiple subzones, we assume that an escort is needed for every zone in which at least one subzone has sea ice thickness above the ice breaker threshold (Table S1). Based upon this, we apply the appropriate tariff to a given shipment, multiplying the per-tonnage tariff (Table S3) by the assumed tonnage of the crude oil tankers, which is 70,080 tonnes for 1A vessels and 70,853 tonnes for 1AS vessels. We consider three RUB/USD exchange rates consistent with the Base, High, and Low scenarios established by Theocharis (2024). We also consider a 'discounted fee' scenario in which a fixed icebreaker escort fee of $5/ton is applied to any shipment needing an escort, regardless of the number of zones in which an escort is needed (Theocharis, 2024).

Following the assumptions applied by Theocharis et al. (2024), we assume that both the 1A and 1AS ice class vessels have operating costs of $8,406 per day, and we add a Suez Canal fee of $141,449 to the cost of the Western route. Finally, in the *LowC|2.6* scenario, we incorporate the costs associated with CO_2 emissions by multiplying the CO_2 prices per unit of emission from the GCAM results (Table S2) by the emissions for the specific shipping vessel and route.

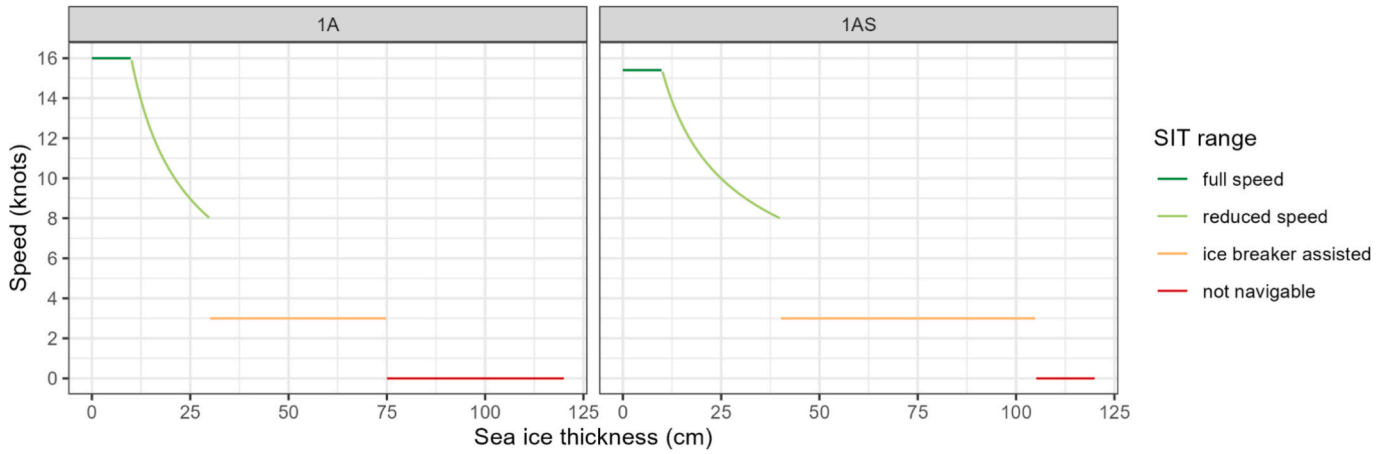

Fig. 5. Speed as a function of sea ice thickness for 1A and 1AS vessels. Source: authors' simulations based upon the speed rules defined by Faury and Cariou (2016); Cheaitou et al (2016), and Faury et al (2020).

3.6. Route choice, number of trips, and emissions

For each subAU, we determine the route over which oil produced in a given month will be shipped based on navigability and cost (Fig. 3). First, if any NSR subzone to the east and/or west of the subAU has an average SIT above the navigability threshold, we assume that none of the oil can be shipped via the East and/or West route, respectively. If both routes are navigable, we determine the proportion (P) shipped over the East route based on the relative total costs of each route using the following logit choice function, where $C_{East,a,r,m,y,v}$ and $C_{West,a,r,m,y,v}$ are the costs of shipping oil from subAU a over the East and West routes, respectively, during month m of year y under RCP r (2.6 or 8.5) using vessel type v (equation 4). The logit exponent parameter used here (−0.5) produces a distribution of route choice within the range of cost differentials in this analysis.

$$P_{East,a,r,m,y,v} = \frac{exp(-0.5{*}C_{East,a,r,m,y,v})}{exp(-0.5{*}C_{East,a,r,m,y,v}) + exp(-0.5{*}C_{West,a,r,m,y,v})} \quad [4]$$

We assume that the remainder of the oil produced is shipped over the West route. We then calculate the resulting number of outbound trips in each direction needed from each subAU over time using the assumption that 1A and 1AS vessels can carry 70,080 tonnes and 70,853 tonnes of oil, respectively (Faury et al., 2020). We make the simplifying assumption that all shipments will use the same route (either East or West) for the return (unloaded) leg as for the outbound (loaded with cargo) leg. We calculate the CO_2 emissions from 1A and 1AS vessels associated with each trip using Equation 5, where $E_{r,m,y,d,v}$ is the total CO_2 emissions from ship type v in direction d during month m of year y under RCP r, Z are the NSR subzones that must be crossed, $F_{z,r,m,y,v}$ is the amount of fuel consumed in subzone $z \in Z$, c is the CO_2 emissions coefficient, and $F_{o,d}$ is the amount of fuel consumed outside the NSR in direction d. We assume a CO_2 emissions coefficient of 3,206 kg CO_2/ton of fuel consumed, which is consistent with the value used by Wang et al. (2020) and Cheaitou et al. (2022) for vessels using very low sulfur fuel oil (VLSFO) on the NSR, based on Corbett et al. (2010). Emissions in equation 5 are multiplied by 2 to account for both the outbound and return legs.

$$E_{r,m,y,d,vt} = 2{*}\left[\sum_{z \in Z}(F_{z,r,m,y,vt}{*}c) + (F_{o,d}{*}c)\right] \quad [5]$$

While the current Russian icebreaker fleet still includes some diesel and diesel-electric vessels, there is an ongoing transition to a nuclear fleet, with 9 of 13 total fleet icebreakers planned to be nuclear-powered by 2030 (High North News, 2022). Therefore, we do not associate fossil fuel use and resulting CO2 emissions with ice breakers in this analysis and instead assume that only nuclear icebreakers will be used.

4. Results

4.1. NSR navigability

We find increasing navigability of the NSR over time as sea ice thins, at a faster pace under RCP 8.5 (used in the *BAU|8.5* scenario) compared to under RCP 2.6 (used in the *BAU|2.6* and *LowC|2.6* scenarios) (Fig. 7). Under RCP 8.5, multiple ensemble members project year-round navigability starting in about 2070 for 1A vessels and 2065 for 1AS vessels and, by the end of the century, most ensembles project navigability for both vessel types during 10 to 12 months. However, under RCP 2.6, navigability increases more slowly and the NSR is projected to be navigable for only about 5 months for 1A vessels and 7 months for 1AS vessels at the end of the century.

4.2. "Stranded" offshore oil production

Due to varying navigability conditions along the NSR, we find that there are certain months when neither of the routes are projected to be accessible to ship oil produced in a given subAU (Fig. 8). This occurs when at least one subzone to the east and at least one subzone to the west of the subAU has projected SIT above the navigability threshold. In reality, it is possible that this oil could be stored and shipped when conditions are more favorable. However, given infrastructure uncertainties, we make the simplifying assumption that this oil will not be shipped on the NSR (e.g., it will be transported by land), thereby excluding any "stranded" oil from the remainder of our shipping analysis.

4.3. Route choice and shipping volumes

In our scenarios, the remainder of oil produced (i.e., not stranded) is shipped to the destination port of Dongjiakou, China. The shipments are split between the East and West routes based on both navigability and cost-based economic choice. Results are presented first using the baseline method to calculate ice breaker escort fees (official NSRA fees with the Base RUB/USD exchange rate), and fee sensitivity cases are assessed in Section 4.6. Fig. 9 shows the proportion of oil produced for which both routes are navigable and route choice is determined by cost. On an annual basis, about 30% of oil produced can be shipped in either direction under current SIT conditions; depending on vessel type, this share increases to about 50–60% in the *BAU|2.6* and *LowC|2.6* scenarios and nearly 100% in the *BAU|8.5* scenario by 2100. Most of the remaining oil can only be shipped via the West route, with a small

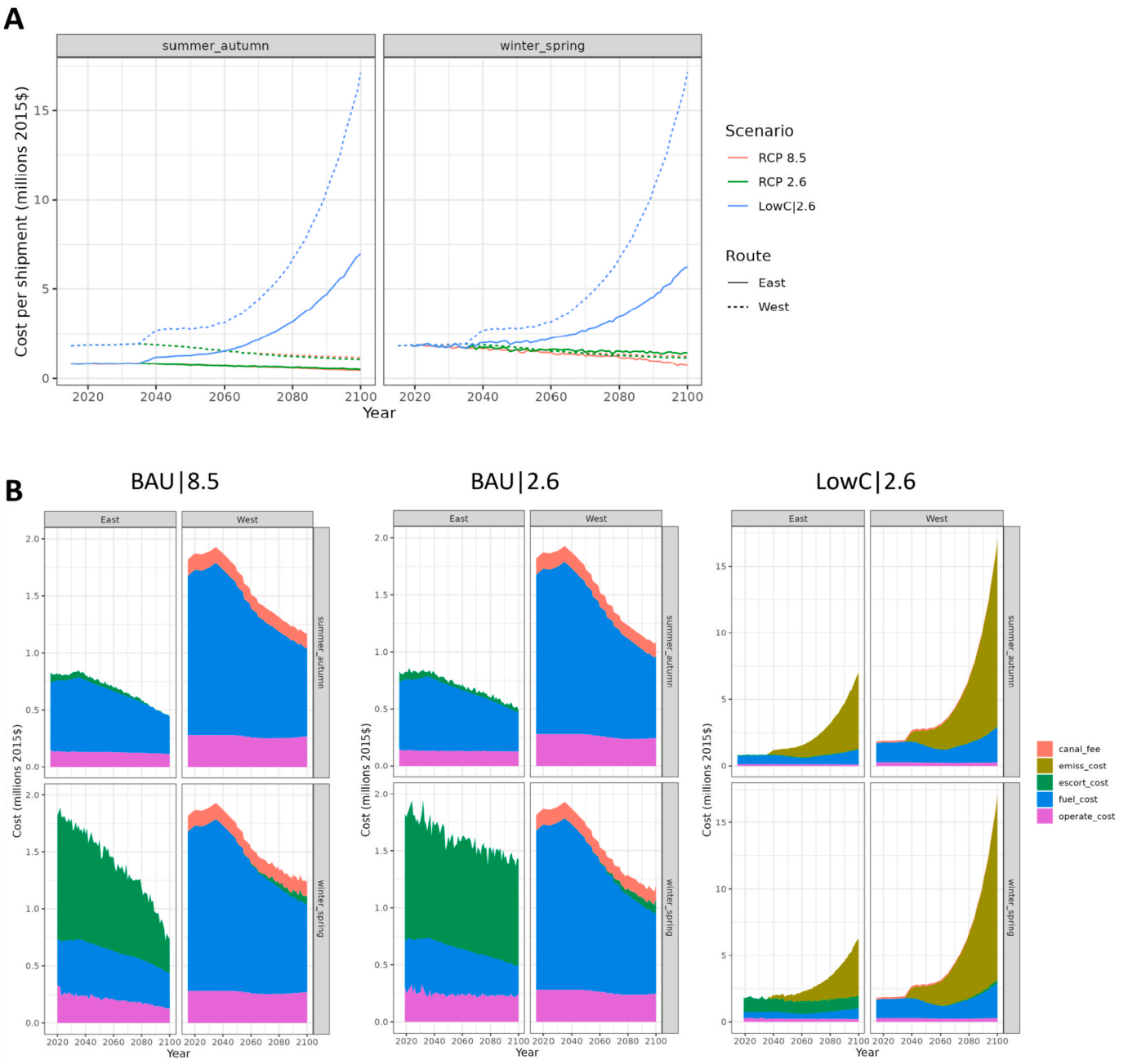

Fig. 6. Summary of average (A) total costs and (B) average costs by source per oil shipment on each route in summer/autumn (July through November) versus winter/spring (December through June) for a 1AS ship. Note that in (B) the y-axis scale differs between LowC|2.6 and the other two scenarios.

"stranded" proportion not able to be shipped in either direction as discussed in Section 4.2 (Fig. 8). The share of shipments for which both routes are navigable is much lower and varies more between scenarios in the winter and spring compared to the summer and autumn (Fig. 9).

For both ship types, eastbound oil shipments increase the most rapidly in the *BAU|8.5* scenario, surpassing westbound shipments by 2070 for 1AS ships and 2085 for 1A ships (Fig. 10). Since most of the oil is produced toward the Western end of the Russian Arctic throughout the century (Fig. S2), these eastbound shipments generally traverse a longer portion of the NSR compared to westbound shipments, but an overall shorter distance to their destination port. By the end of the century, the total amount of oil shipped is similar in *LowC|2.6* and *BAU|8.5*. Compared to *BAU|8.5*, however, shipping decisions in *LowC|2.6* incorporate two offsetting impacts: thicker sea ice increases relative ice breaker escort costs, fuel costs, and operation costs on the East route, while the higher costs of CO_2-emitting fuels increase relative costs on the longer West route (Fig. 6). The former effect is stronger, particularly for 1A vessels, resulting in a lower proportion of oil shipped on the East route in *LowC|2.6* compared to *BAU|8.5* (Fig. 10). The *BAU|2.6* scenario, which has thicker sea ice than *BAU|8.5*, but not the added emissions costs that are in the *LowC|2.6* scenario, results in the least total oil shipments and the lowest proportion shipped on the East route, with the West route still contributing the majority of oil shipped by 2100 (Fig. 10). Overall, the 1AS vessel type results in more oil shipped on the East route and less on the West route across scenarios, compared to 1A. The largest difference between the 1A and 1AS results occurs in the LowC|2.6 scenario. The combination of relatively high oil production and relatively high sea ice thickness makes vessel ice class particularly influential in this scenario. See Fig. S3 for projected oil shipments for all CMIP6 ensembles.

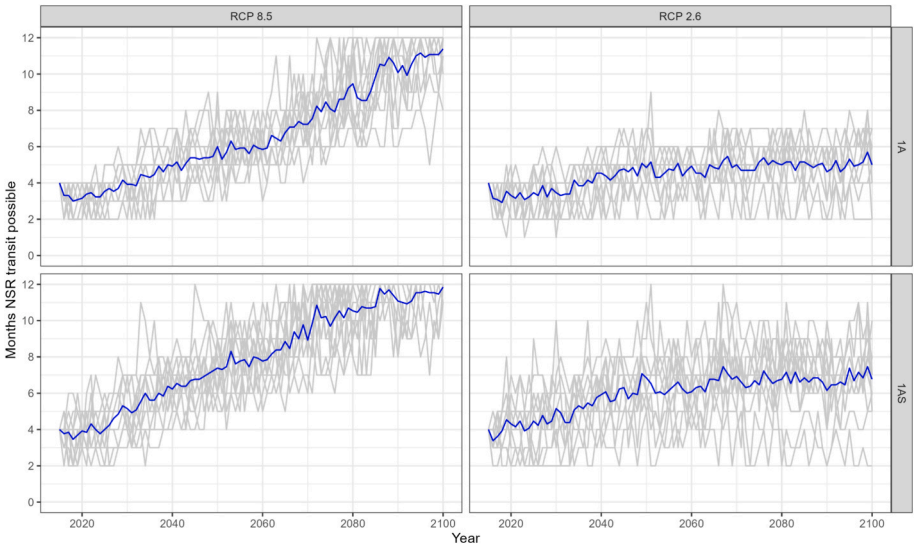

Fig. 7. Months per year when the entire NSR transit is possible for vessel types 1A and 1AS, meaning that sea ice thickness in all subzones is below the ships' respective navigability thresholds, under RCP 8.5 and RCP 2.6 sea ice thickness projections. All CMIP6 ensembles are shown in grey and the ensemble average is shown in blue.

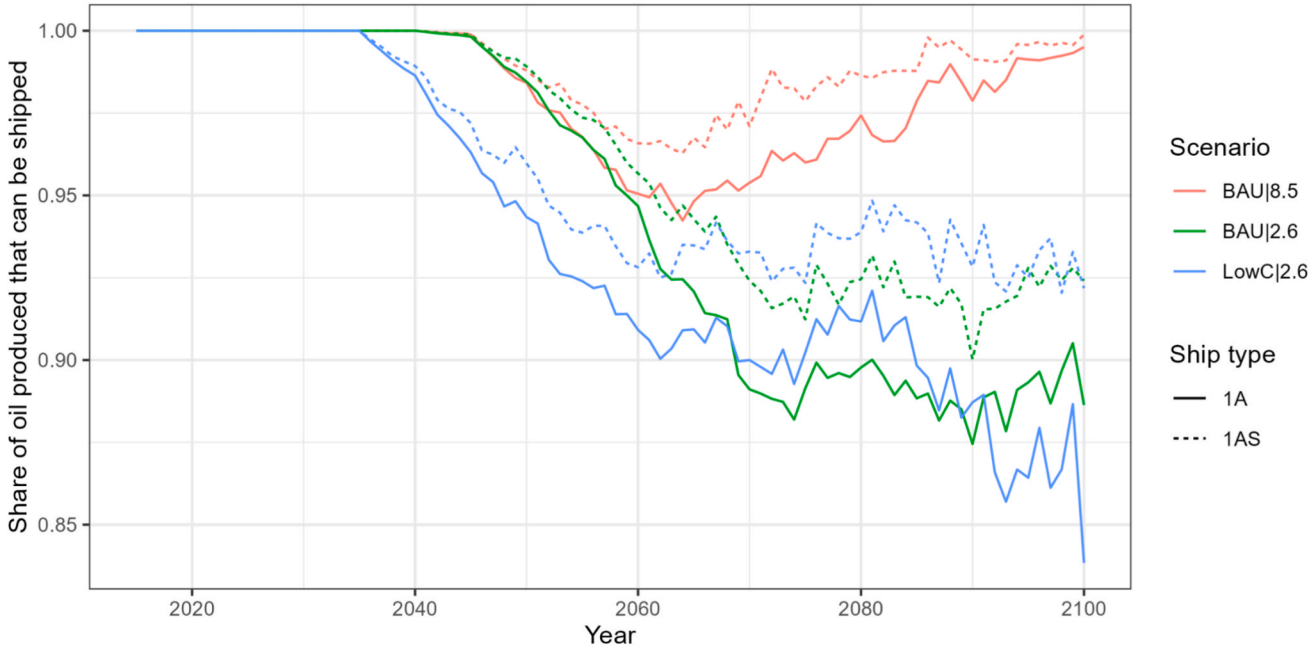

Fig. 8. Share of oil produced each year that can be shipped on the NSR (i.e., at least one of the two routes are projected to be navigable). Note that in each scenario, only one vessel type (either 1A or 1AS) is used.

4.4. Shipping traffic

Growth in the volume of offshore oil shipped from the Russian Arctic results in increasing shipping traffic on the NSR from both eastbound and westbound shipments. The number of eastbound trips increases through the century in all scenarios, with *BAU|8.5* exhibiting the most rapid growth and reaching around 300–350 trips per year by 2100 depending on vessel type used (Tables 3 and S4). Eastbound trips increase more slowly in *BAU|2.6*, reaching about 50–100 trips per year. As with tonnage of oil shipped, there are more eastbound trips and fewer westbound trips when 1AS vessels are used compared to 1A vessels (Tables 3 and S4).

The total shipping traffic within the NSR, measured in ship-km and encompassing both eastbound and westbound shipments, provides additional insight into the evolution of total NSR traffic (Fig. 11) and the spatial distribution of this traffic among subzones (Fig. 12). These traffic patterns are influenced by the distribution of oil production across AUs as well as the directions in which shipments travel within the NSR based on the economic choice model. Shipping traffic remains relatively low and consistent across scenarios through the mid-century, with traffic concentrated at the western end of the NSR. From 2050 to 2070, shipping traffic is greatest in the *LowC|2.6* scenario and the traffic distribution in all scenarios begins to shift westward. By the end of the century, *BAU|8.5* results in the most total NSR shipping traffic followed by *LowC|2.6*, with traffic distributed relatively evenly along the route in both scenarios. NSR traffic in the *BAU|2.6* scenario remains concentrated at the western end of the route through 2100 with much lower total traffic. These trends are consistent between vessel types, although

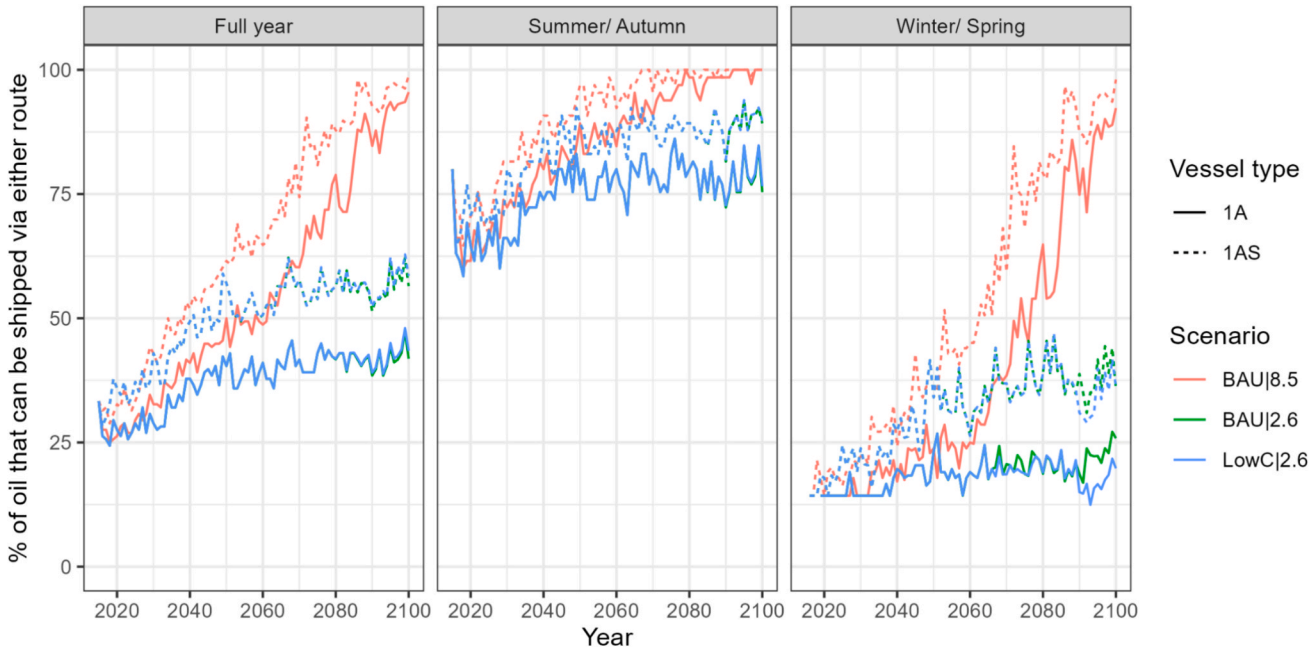

Fig. 9. Ensemble average proportion of Russian Arctic offshore oil produced that can be shipped on either route due to navigable sea ice conditions, shown both on an annual basis and seasonally.

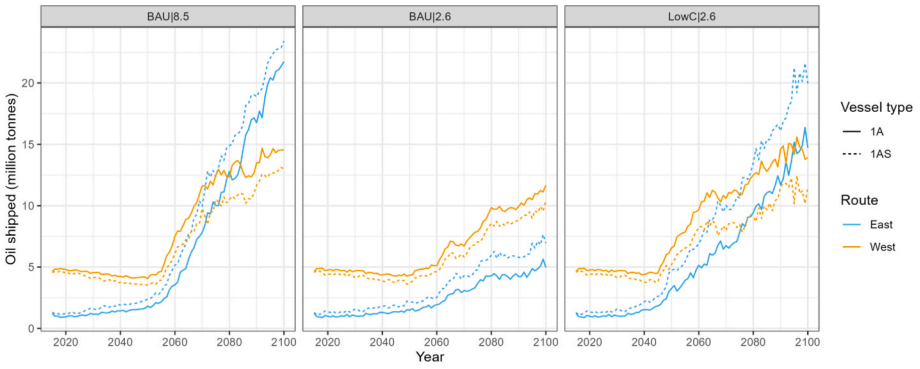

Fig. 10. Ensemble average tonnage of Russian Arctic offshore crude oil shipped eastwards along the NSR or westwards towards the SCR in the BAU|8.5, BAU|2.6, and LowC|2.6 scenarios for 1A and 1As vessels. Note that in each scenario, only one vessel type (either 1A or 1AS) is used. The Base USD/RUS exchange rate is applied to icebreaker escort fees in the cost projections used here.

Table 3
Summary of NSR navigability, oil production, and resulting number of eastbound and westbound trips for a 1A vessel across scenarios and years. The same data are given for a 1AS vessel in Table S4.

Year	Scenario	Months open*	Oil produced (Mt)	Oil shipped (Mt)	Oil stranded (Mt)	Trips East	Trips West	Total Trips
2025	BAU|2.6	3.5	5.73	5.7	0	14.7	67	81.7
	BAU|8.5	3.5	5.73	5.7	0	14.9	66.8	81.7
	LowC|2.6	3.5	5.73	5.7	0	14.7	67	81.7
2050	BAU|2.6	4.8	5.92	5.8	0.093	21.1	62.1	83.2
	BAU|8.5	6	5.98	5.9	0.095	26	58	84
	LowC|2.6	4.8	10.37	9.8	0.55	46.6	93.5	140.1
2075	BAU|2.6	5.2	12.79	11.6	1.204	52.5	112.9	165.4
	BAU|8.5	8.1	23.39	22.5	0.89	142.9	178.2	321.1
	LowC|2.6	5.2	20.54	18.7	1.883	112.3	154	266.3
2100	BAU|2.6	5	18.5	16.6	1.876	70.7	166.5	237.2
	BAU|8.5	11.4	36.44	36.3	0.147	310.2	207.7	517.9
	LowC|2.6	5	34.05	28.6	5.41	210.1	198.6	408.7

*Number of months during which all subzones of the NSR are navigable.

overall NSR shipping traffic is higher when 1AS ships are used compared to 1A ships (Fig. 11) due to a higher proportion of eastbound trips (Tables 3 and S4). Across scenarios, projected oil tanker shipping traffic to carry the projected offshore oil reaches about 1–3.5 million ship-km by 2100. This could remain a small fraction of the total shipping traffic in the entire Arctic Polar Code area, which was 24 million ship-km

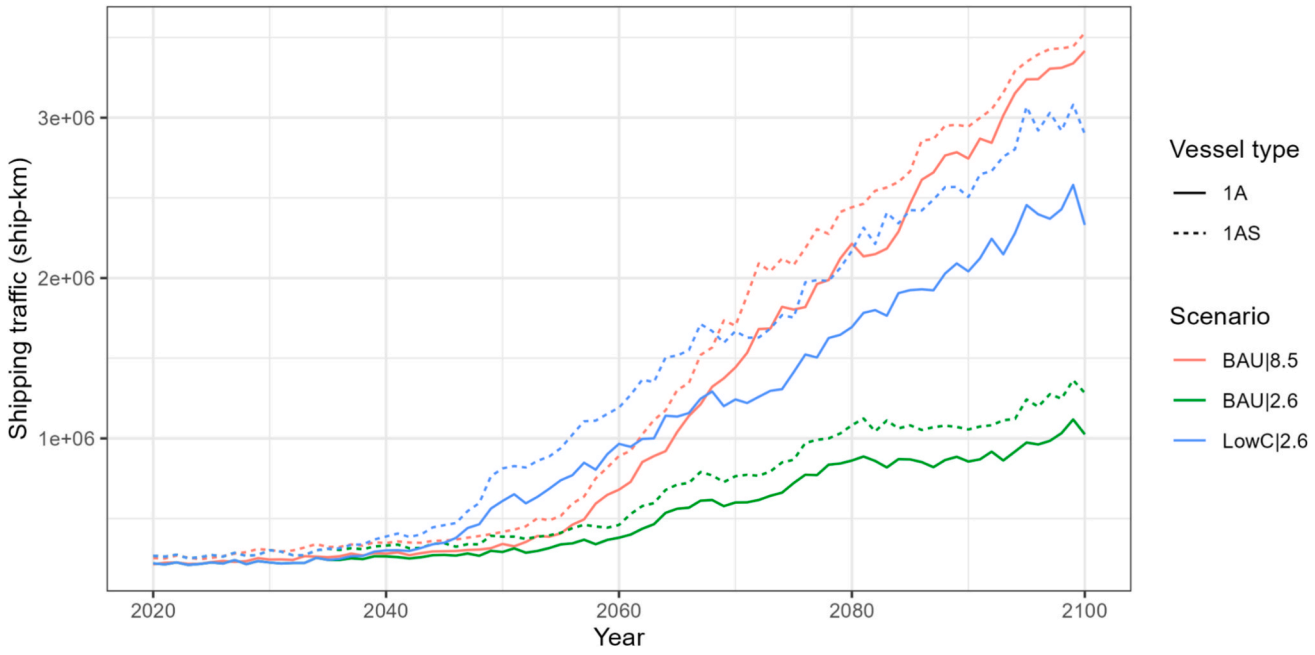

Fig. 11. Total oil tanker shipping traffic to carry projected Russian Arctic offshore oil production on the NSR resulting from offshore oil shipments (ensemble average ship-km). Note that in each scenario, only one vessel type (either 1A or 1AS) is used. The Base USD/RUS exchange rate is applied to icebreaker escort fees in the cost projections used here.

in 2023 (Arctic Council, 2024). However, when focusing on transit voyages traversing the NSR to reach destinations outside of the Arctic, the projected 70–300 additional trips per year by 2100 could contribute significantly to the growth of this type of shipping traffic; there were 97 total NSR transit voyages in 2024, of which only 18 carried crude oil (Centre for High North Logistics, 2024).

4.5. Emissions

Increasing NSR shipping traffic will have important implications for CO_2 emissions. For each oil shipment, we account for emissions occurring both inside and outside of the NSR to reach the destination port. The 1AS vessel class results in consistently higher total CO_2 emissions than the 1A vessel class throughout the century since 1AS vessels consume more fuel; however, overall trends are similar for 1A vessels (Fig. 13) and 1AS vessels (Fig. S5). By the end of the century, total CO_2 emissions from shipping Russian Arctic offshore oil are similar in the *BAU|8.5* and *LowC|2.6* scenarios and lower in the *BAU|2.6* scenario (Fig. 13). In the *BAU|8.5* scenario, emissions resulting from westbound trips begin to level out around 2070 while emissions from eastbound trips continue to grow starting in the mid-century. In the other two scenarios, however, emissions from trips in both directions increase consistently (Fig. 13).

Even though the number of eastbound trips reaches or exceeds the number of westbound trips by 2100 in both *BAU|8.5* and *LowC|2.6*, westbound trips still contribute the majority of emissions. This is due to the much longer transit outside the NSR required by the West route (around Europe, through the Mediterranean, the Suez Canal, and the Indian & South China Seas) compared to the East route (through the Bering strait and down the East Asian coast). This also means that most of the CO_2 emissions resulting from westbound trips occur outside the NSR while a higher proportion of emissions from eastbound trips occur within the NSR (Fig. 13). For both vessel types, the average emissions intensity of shipping oil (i.e., the amount of CO_2 emissions per tonne of oil shipped) is lowest in the *BAU|8.5* scenario by the end of the century while it is highest in the *BAU|2.6* scenario; westbound shipments are consistently more emissions intensive than eastbound shipments, and 1AS vessels have higher emissions intensities than 1A vessels (Fig. S6), again due to higher fuel consumption.

4.6. Ice breaker escort fee sensitivities

The discounted ($5/ton) ice breaker escort fee case and the low RUB/USD rate case result in lower costs per shipment compared to the base RUB/USD rate case, while the high RUB/USD rate case results in higher costs (Fig. S7). The largest cost differences are seen for shipments on the East route in the winter/spring season since these shipments require the most ice breaker escorts. However, the difference in route choice and resulting NSR traffic (Fig. 14) is relatively small, with an ensemble average of up to 3% higher NSR traffic in the discounted fee case and up to 5% lower traffic in the high RUB/USD exchange rate case. This small difference in route choice, despite relatively large cost differences in some cases, can be explained by three dynamics. First, substantial cost differences only occur for eastbound shipments in the winter and spring (Fig. S7), since these are the shipments for which icebreaker escort fees make up a large proportion of total costs (Fig. 6). Second, the fee differences only impact route choice when both routes are navigable; the proportion of shipments for which this is the case in the winter/spring season is limited, especially in the early-mid century and for the *BAU|2.6* and *LowC|2.6* scenarios (Fig. 9). Third, the logit choice economic framework used in our cost model introduces some inelasticity into route choice, wherein a distribution of route choice is assumed for any given absolute difference between costs.

5. Discussion and conclusions

Our results align with the growing literature showing that the NSR will become increasingly navigable for a larger portion of the year throughout the century as sea ice thickness declines under both RCP 8.5 and RCP 2.6 (Aksenov et al., 2017; Stephenson et al., 2014; Stephenson et al., 2013). Considering the costs of fuel, icebreakers, and operations, our analysis suggests that over the century and particularly in the high-warming *BAU|8.5* scenario, the NSR will become navigable and cost-competitive with the alternative Suez Canal route for shipping oil produced in the offshore Russian Arctic to East Asian markets. These findings are consistent between two vessel classes, and they agree with other studies highlighting the potential economic benefits of the NSR for bulk shipping (Kavirathna & Shibasaki, 2021; Cheaitou et al., 2020).

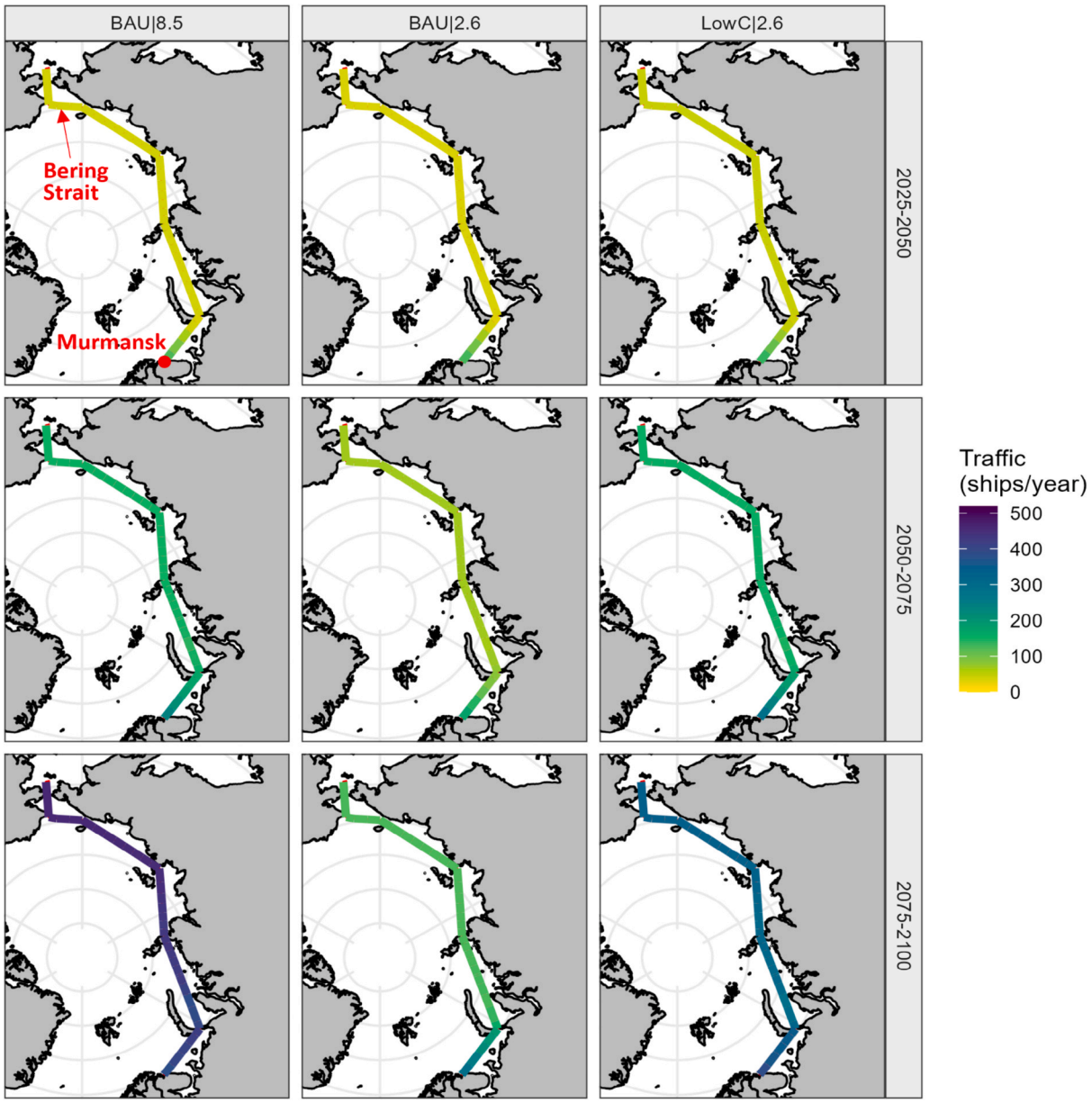

Fig. 12. Oil tanker traffic required to carry projected Russian Arctic offshore oil production along the NSR by scenario during the short-term (2025–2050), mid-term (2050–2075), and long-term (2075–2100), accounting for both outbound and return trips of class 1A vessels. Fig. S4 shows these data for class 1AS vessels. The Base USD/RUS exchange rate is applied to icebreaker escort fees in the cost projections used here.

Beyond overall NSR navigability and cost-competitiveness, our analysis projects the potential quantity of shipments on the NSR resulting specifically from increasing production of Arctic offshore oil. This is a key addition to the literature since natural resource extraction is expected to be a prominent source of Arctic shipping growth (Arctic Council, 2024). We also project changes in the spatial distribution of this shipping traffic, which remains concentrated at the western end of the NSR in *BAU|2.6* compared to a more even distribution in the other scenarios by the end of the century. The spatial distribution of shipping traffic is important in the Arctic context due to the need to plan strategic port infrastructure development (Gunnarsson, 2021; Herman et al., 2022) and the need to understand potential albedo effects of ships' particulate matter emissions such as black carbon (Zhang et al., 2019; Sand et al., 2013).

We find that the increased use of the eastbound NSR route as an alternative to the westbound Suez Canal route can lower the CO_2 emissions intensity of shipping since the eastbound route is shorter and uses less fuel. In our scenarios, eastbound trips had about 58% lower CO_2 emissions compared to westbound trips. This finding agrees with other work highlighting the greenhouse gas emissions reduction potential of shipping on the NSR (Wang et al., 2021). However, this decrease in total CO_2 emissions is also accompanied by an increasing proportion of emissions occurring within the NSR. This could have nuanced implications for Arctic ice coverage, since particulate matter emissions from shipping, which occur alongside CO_2 emissions, may have disproportionate albedo effects in the Arctic (Lindstad et al., 2016).

In addition to assessing the impacts of projected sea ice thickness on Arctic offshore oil production and shipping costs, we also consider the impacts of an emission scenario consistent with RCP 2.6 on both oil production and route choice in the *LowC|2.6* scenario. This scenario represents a future with a relatively high demand for Arctic offshore oil in dynamic global energy markets (Zhang et al., 2024) and relatively low climate impacts on SIT. In this scenario, there is also an additional cost associated with CO_2 emissions in line with RCP 2.6. This raises the costs

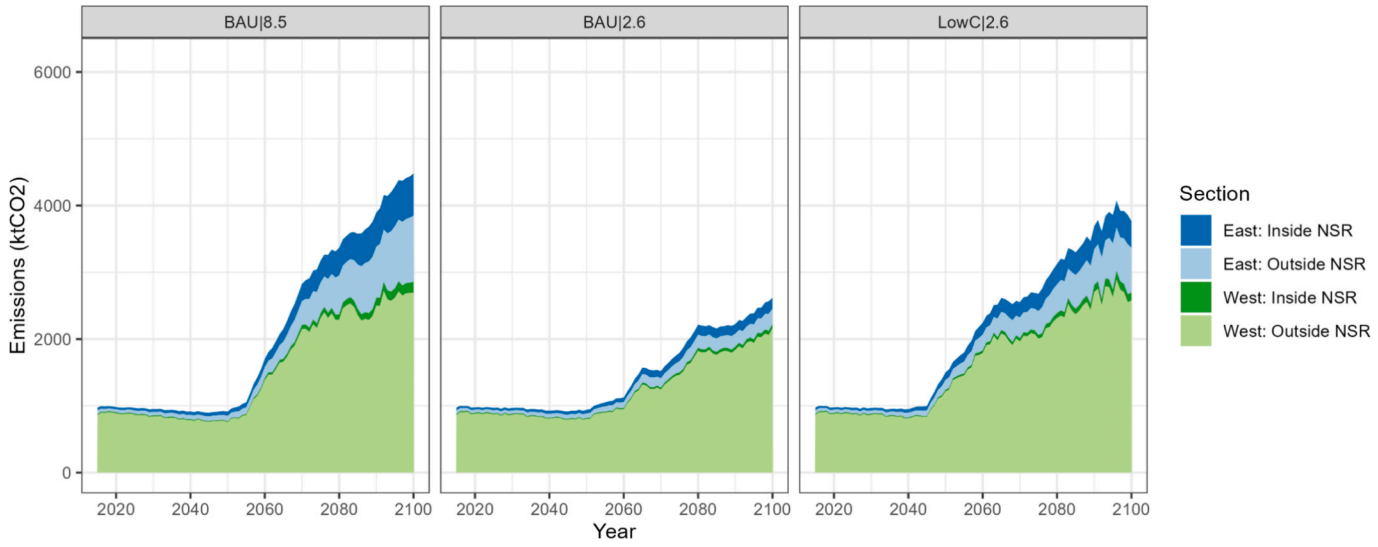

Fig. 13. Projected total CO_2 emissions from shipping Arctic Russian offshore oil with class 1A vessels. Totals include emissions from both the within-NSR and outside-NSR portions of both eastbound and westbound trips. Fig. S5 shows these data for class 1AS vessels. The Base USD/RUS exchange rate is applied to icebreaker escort fees in the cost projections used here.

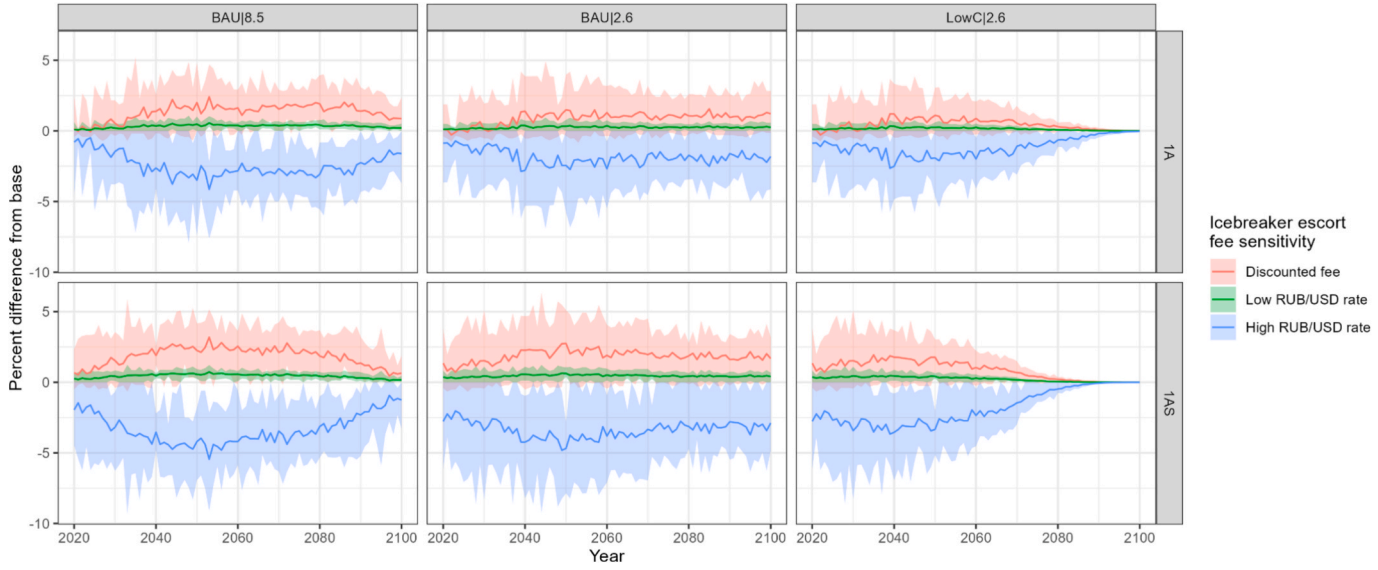

Fig. 14. Percent difference in total oil tanker shipping traffic on the NSR resulting from offshore oil shipments (ship-km) in the three icebreaker escort sensitivity cases (discounted fee, low RUB/USD rate, and high RUB/USD rate) compared to the base RUB/USD rate case. The lines represent climate model ensemble averages and the shaded regions represent the range of ensembles.

associated with shipping, due to the additional cost on fuels that produce emissions. Sustained high SIT increases the competitiveness of the more ice-free West route while the higher costs of CO_2– emitting fuels partially counteracts this effect by increasing the competitiveness of the shorter East route. The effect of the higher fuel costs aligns with previous studies finding that a carbon tax could make the NSR more economically attractive compared to the Suez Canal Route (Cariou & Faury, 2015).

Our analysis contributes to the growing literature projecting impacts of future sea ice decline and socioeconomic factors on shipping potential over the NSR (Lasserre, 2014; Khon et al., 2017; Faury et al., 2020; Gleb and Jin, 2021). Future shipping traffic on the NSR will also depend on the characteristics of and markets for specific goods to be shipped. Our analysis addresses this by incorporating long-term projections of Arctic offshore oil production volumes from a global human-Earth system model (GCAM) and exploring the extent to which this oil could contribute to NSR shipping traffic. Further, while previous models of NSR cost competitiveness have assessed the impacts of varying key economic factors like fuel prices in addition to projected sea ice thickness, most of these economic components have been treated as independent variables or sensitivity cases. We add novel insights to the literature by leveraging GCAM to integrate dynamic and internally consistent projections of Arctic offshore oil production, fuel prices, and emissions pathways, in addition to SIT, into our shipping cost model. These socioeconomic factors are not treated as independent variables, but instead are endogenously modeled in GCAM, allowing them to vary in response to the evolving conditions in each scenario. This approach captures the inherent feedback and cross-dependencies between fuel prices, oil shipment volumes, and emissions costs, all of which are projected under consistent scenarios of future sea ice thickness change and global energy system evolution. Therefore, our study offers a more rigorous and internally consistent understanding of how economic factors evolve dynamically across different future scenarios and the

associated effects on Arctic shipping of a key commodity.

Our key limitation of our methodology, which could be addressed in future work to further develop the analysis, is that our shipping model focuses on SIT dynamics along a fixed NSR channel; we do not incorporate projections of SIT outside of this route. While many of the AUs intersect with or are in close proximity to the NSR, some extend into higher latitudes (Fig. 2). Since we assume that oil shipments begin at the subzones of the NSR with which the AUs intersect longitudinally, our analysis does not take into account potential navigability constraints and fuel consumption associated with traveling from the point of extraction to the corresponding NSR subzone. A more dynamic route choice approach, allowing shipments to take a least-cost path from the point of extraction to the destination rather than a fixed path, could be more realistic in future research. However, our approach represents an insightful step towards an integrated human-Earth systems approach to modeling future Arctic shipping, especially given the lack of certainty on points of extraction within AUs that are not yet in production.

Our approach could also be expanded in future work to incorporate additional commodities that could be shipped through the Arctic such as liquefied natural gas (Meza et al., 2023), additional Arctic shipping routes, other vessel types, and other emissions species such as black carbon. Future work could also assess shipping cost factors not included here, such as high insurance costs for vessels navigating in the Arctic (Sarrabezoles et al., 2016) and other environmental constraints on shipping, such as fog (Song et al., 2023; Wang et al., 2023).

Funding

This research was funded as part of the Interdisciplinary Research for Arctic Coastal Environments (InteRFACE) project through the Department of Energy, Office of Science, Biological and Environmental Research Earth and Environmental Systems Sciences Division Multi-Sector Dynamics program. Awarded under contract Grant # 89233218CNA000001 to Triad National Security, LLC ("Triad").

CRediT authorship contribution statement

Taryn Waite: Writing – review & editing, Writing – original draft, Visualization, Validation, Software, Formal analysis, Data curation. **Siwa Msangi:** Writing – review & editing, Writing – original draft, Visualization, Validation, Supervision, Software, Methodology, Investigation, Data curation, Conceptualization. **Ying Zhang:** Writing – review & editing, Writing – original draft, Data curation. **Molly French:** Visualization, Formal analysis, Data curation. **Nazar Kholod:** Writing – review & editing, Validation, Data curation. **Jae Edmonds:** Writing – review & editing, Methodology, Investigation, Conceptualization. **Stephanie T. Morris:** Writing – review & editing, Writing – original draft, Supervision, Resources, Project administration, Investigation, Conceptualization.

Declaration of competing interest

The authors declare that they have no known competing financial interests or personal relationships that could have appeared to influence the work reported in this paper.

Appendix A. Supplementary data

Supplementary data to this article can be found online at https://doi.org/10.1016/j.trip.2026.101841.

Data availability

The data and code used to produce this analysis can be found online at https://github.com/trwaite/NSR_shipping_model.

References

Aksenov, Y., Popova, E.E., Yool, A., Nurser, A.J.G., Williams, T.D., Bertino, L., Bergh, J., 2017. On the future navigability of Arctic sea routes: High-resolution projections of the Arctic Ocean and sea ice. Mar. Policy 75, 300–317. https://doi.org/10.1016/j.marpol.2015.12.027.

Arctic Council, 2024. "Arctic shipping update: 37% increase in ships in the Arctic over 10 years. https://arctic-council.org/news/increase-in-arctic-shipping/.

Bauer, N., Bosetti, V., Hamdi-Cherif, M., Kitous, A., McCollum, D., Méjean, A., Rao, S., Turton, H., Paroussos, L., Ashina, S., Calvin, K., Wada, K., van Vuuren, D., 2015. CO2 emission mitigation and fossil fuel markets: dynamic and international aspects of climate policies. Technol. Forecast. Soc. Chang. 90 (PA), 243–256. https://doi.org/10.1016/J.TECHFORE.2013.09.009.

Box, J.E., Colgan, W.T., Christensen, T.R., Schmidt, N.M., Lund, M., Parmentier, F.W., Brown, R., Bhatt, U.S., Euskirchen, E.S., Romanovsky, V.E., 2019. Key indicators of Arctic climate change: 1971-2017. Environ. Res. Lett. 14. https://doi.org/10.1088/1748-9326/aafc1b.

Calvin, K., Patel, P., Clarke, L., Asrar, G., Bond-Lamberty, B., Cui, R.Y., Di Vittorio, A., Dorheim, K., Edmonds, J., Hartin, C., Hejazi, M., Horowitz, R., Iyer, G., Kyle, P., Kim, S., Link, R., McJeon, H., Smith, S.J., Snyder, A., Waldhoff, S., Wise, M., 2019. GCAM v5.1: Representing the linkages between energy, water, land, climate, and economic systems. Geosci. Model Dev. 12, 677–698. https://doi.org/10.5194/gmd-12-677-2019.

Cariou, P., Faury, O., 2015. Relevance of the Northern Sea Route (NSR) for bulk shipping. Transp. Res. A Policy Pract. 78, 337–346. https://doi.org/10.1016/j.tra.2015.05.020.

Centre for High North Logistics, 2024. "Main Results of NSR Transit Navigation in 2024). Retrieved from https://chnl.no/news/main-results-of-nsr-transit-navigation-in-2024/.

Cheaitou, A., Faury, O., Cariou, P., Hamdan, S., Fabbri, G., 2019. Ice thickness data in the northern sea route (NSR) for the period 2006–2016. Data Brief 24. https://doi.org/10.1016/j.dib.2019.103925.

Cheaitou, A., Faury, O., Cariou, P., Hamdan, S., Fabbri, G., 2020. Economic and environmental impacts of Arctic shipping: a probabilistic approach. Transp. Res. Part D: Transp. Environ. 89, 102606. https://doi.org/10.1016/J.TRD.2020.102606.

Cheaitou, A., Faury, O., Etienne, L., Fedi, L., Rigot-Muller, P., Stephenson, S., 2022. Impact of CO2 emission taxation and fuel types on Arctic shipping attractiveness. Transp. Res. D 112. https://doi.org/10.1016/j.trd.2022.103491.

Chen, J., Kang, S., Chen, C., You, Q., Du, W., Xu, M., Zhong, X., Zhang, W., Chen, J., 2020. Changes in sea ice and future accessibility along the Arctic Northeast Passage. Global Planet. Change 195, 103319. https://doi.org/10.1016/j.gloplacha.2020.103319.

Chen, Y., Lu, J., Ma, M., 2022. How does oil future price imply bunker price—cointegration and prediction analysis. Energies 15, 3630. https://doi.org/10.3390/en15103630.

Christensen, M., Georgati, M., Arsanjani, J.J., 2019. A risk-based approach for determining the future potential of commercial shipping in the Arctic. J. Marine Eng. & Technol. 21 (2), 82–99. https://doi.org/10.1080/20464177.2019.1672419.

Corbett, J.J., Lack, D.A., Winebrake, J.J., Harder, S., Silberman, J.A., Gold, M., 2010. Arctic shipping emissions inventories and future scenarios. Atmos. Chem. Phys. 10, 9689–9704. https://doi.org/10.5194/acp-10-9689-2010.

Erikstad, S.O., Ehlers, S., 2012. Decision support framework for exploiting northern sea route transport opportunities. Ship Technol. Res. 59 (2), 34–42. https://doi.org/10.1179/str.2012.59.2.003.

Faury, O., Cheaitou, A., Givry, P., 2020. Best maritime transportation option for the Arctic crude oil: a profit decision model. Transp. Res. Part E 136, 101865. https://doi.org/10.1016/j.tre.2020.101865.

Faury, O., Cariou, P., 2016. The Northern Sea Route competitiveness for oil tankers. Transp. Res. Part A 94, 461–469. https://doi.org/10.1016/j.tra.2016.09.026.

Gleb, S., Jin, J.G., 2021. Evaluating the feasibility of combined use of the Northern Sea Route and the Suez Canal Route considering ice parameters. Transp. Res. Part A 147, 350–369. https://doi.org/10.1016/j.tra.2021.03.024.

Gunnarsson, B., 2021. Recent ship traffic and developing shipping trends on the Northern Sea Route–Policy implications for future arctic shipping. Mar. Policy 124, 104369. https://doi.org/10.1016/j.marpol.2020.104369.

Hermann, R.R., Lin, N., Level, J., Kovalenko, A., 2022. Arctic transshipment hub planning along the Northern Sea Route: a systematic literature review and policy implications of Arctic port infrastructure. Mar. Policy 145, 105275. https://doi.org/10.1016/j.marpol.2022.105275.

Humpert, Malte. 2018. Traffic on Northern Sea Route Doubles as Russia Aims to Reduce Ice-class Requirements. High North News. Retrieved from https://www.highnorthnews.com/en/traffic-northern-sea-route-doubles-russia-aims-reduce-ice-class-requirements.

Kavirathna, C.A., Shibasaki, R., 2021. Economic feasibility of Arctic shipping from multiple perspectives: a systematic review. Okhotsk Sea and Polar Oceans Research 5, 15–22.

Khon, V.C., Mokhov, I.I., Semenov, V.A., 2017. Transit navigation through Northern Sea Route from satellite data and CMIP5 simulations. Environ. Res. Lett. 12 (2), 024010. https://doi.org/10.1088/1748-9326/aa5841.

Kwok, R., 2018. Arctic sea ice thickness, volume, and multiyear ice coverage: losses and coupled variability (1958-2018). Environ. Res. Lett. 13. https://doi.org/10.1088/1748-9326/aae3ec.

Lasserre, F., 2014. Case studies of shipping along Arctic routes: Analysis and profitability perspectives for the container sector. Transp. Res. Part A Policy Pract 66, 144–161. https://doi.org/10.1016/j.tra.2014.05.005.

Lazarus, M., van Asselt, H., 2018. Fossil fuel supply and climate policy: exploring the road less taken. Clim. Change 150 (1–2), 1–13. https://doi.org/10.1007/S10584-018-2266-3.

Li, Z., Ding, L., Huang, L., Ringsberg, J.W., Gong, H., Fournier, N., Chuang, Z., 2023. Cost-benefit analysis of a trans-Arctic alternative route to the Suez Canal: a method based on high-fidelity ship performance, weather, and ice forecast models. J. Mar. Sci. Eng. 11 (4), 711. https://doi.org/10.3390/jmse11040711.

Lindstad, H., Bright, R.M., Stromman, A.H., 2016. Economic savings linked to future Arctic shipping trade are at odds with climate change mitigation. Transp. Policy 45, 24–30. https://doi.org/10.1016/j.tranpol.2015.09.002.

Melia, N., Haines, K., Hawkins, E., 2016. Sea ice decline and 21st century trans-Arctic shipping routes. Geophys. Res. Lett. 43, 18. https://doi.org/10.1002/2016GL069315.

Meza, A., Ari, I., Al Sada, M., Koç, M., 2023. Relevance and potential of the Arctic Sea Routes on the LNG trade. Energ. Strat. Rev. 50, 101174. https://doi.org/10.1016/j.esr.2023.101174.

Ministry of Justice of Russia. 2014. "Federal Service for Tariffs, Order of March 4, 2014, N 45-t/1, About the approval of tariffs for the ice breaker escorting of ships rendered by FSUE "ATOMFLOT" in the water area of the Northern Sea Route." http://www.nsra.ru/en/tarrifs_for_icebreaker_escort_atomflot/f79.html.

Notz, D., Community, S.I.M.I.P., 2020. Arctic sea ice in CMIP6. Geophys. Res. Lett. https://doi.org/10.1029/2019GL086749.

Petrik, S., Riemann-Campe, K., Hood, S., Growitsch, C., Schwind, H., Gerdes, R., Rehdanz, K., 2017. Climate change, future Arctic sea ice, and the competitiveness of European Arctic offshore oil and gas production on world markets. Ambio 46, 410–422. https://doi.org/10.1007/s13280-017-0957-z.

Pruyn, J.F.J., van Hassel, E., 2022. The impact of adding the Northern sea route to the Belt and Road Initiative for Europe: a chain cost approach. Transp. Res. Interdiscip. Perspect. 15, 100659. https://doi.org/10.1016/j.trip.2022.100659.

Sand, M., Berntsen, T.K., Seland, Ø., Kristjánsson, J.E., 2013. Arctic surface temperature change to emissions of black carbon within Arctic or midlatitudes. J. Geophys. Res. Atmos. 118 (14), 7788–7798. https://doi.org/10.1002/jgrd.50613.

Sarrabezoles, A., Lasserre, F., Hagouagn'rin, Z., 2016. Arctic shipping insurance: towards a harmonisation of practices and costs? Polar Rec. 52 (4), 393–398. https://doi.org/10.1017/S0032247414000552.

Shandong Port Group Co., Ltd. 2023. Dongjiakou builds China's largest coastal oil storage facility. Accessed April 2024. Retrieved from http://regional.chinadaily.com.cn/ensd-port/2023-08/25/c_913699.htm.

Sibul, G., Jin, J.G., 2021. Evaluating the feasibility of combined use of the Northern Sea Route and the Suez Canal Route considering ice parameters. Transp. Res. A Policy Pract. 147, 350–369. https://doi.org/10.1016/j.tra.2021.03.024.

Song, S., Chen, Y., Chen, X., Chen, C., Li, K.-F., Tung, K.-K., et al., 2023. Adapting to a foggy future along trans-Arctic shipping routes. Geophys. Res. Lett. 50, e2022GL102395. https://doi.org/10.1029/2022GL102395.

Staalesen, A., 2024. Oil tanker Sturman Skuratov is shipping Russian Arctic oil for Gazprom Neft. article in Barents Observer, 21 June 2024. Retrieved from https://www.thebarentsobserver.com/arctic/seaice-lies-thick-on-the-water-as-russian-oil-tanker-sails-arctic-route-without-icebreaker-escort/118937#.

Theocharis, D., Rodrigues, V.S., Pettit, S., Haider, J., 2019. Feasibility of the Northern Sea Route: the role of distance, fuel prices, ice breaking fees and ship size for the product tanker market. Transp. Res. Part E 129, 111–135. https://doi.org/10.1016/j.tre.2019.07.003.

Theocharis, D., Rodrigues, V.S., Pettit, S., Haider, J., 2024. Feasibility and implications of the Northern Sea Route choice: the role of commodity prices, in-transit inventory, and alternative operational modes for the oil product tanker market. Marit. Policy Manag. 51 (3), 363–391. https://doi.org/10.1080/03088839.2022.2119613.

Wan, Z., Nie, A., Chen, J., Ge, J., Zhang, C., Zhang, Q., 2021. Key barriers to the commercial use of the Northern Sea Route: View from China with a fuzzy DEMATEL approach. Ocean & Coastal Manage. 208. https://doi.org/10.1016/j.ocecoaman.2021.105630.

Wang, D., Ding, R., Gong, Y., Wang, R., Wang, J., Huang, X., 2020. Feasibility of the Northern Sea Route for oil shipping from the economic and environmental perspective and its influence of China's oil imports. Mar. Policy 118. https://doi.org/10.1016/j.marpol.2020.104006.

Wang, K., Zhang, Y., Chen, C., Song, S., Chen, Y., 2023. Impacts of Arctic Sea fog on the change of route planning and navigational efficiency in the northeast passage during the first two decades of the 21st century. J. Mar. Sci. Eng. 11, 2149. https://doi.org/10.3390/jmse11112149.

Wang, S., Meng, Q., 2012. Sailing speed optimization for container ships in a liner shipping network. Transp. Res. Part E: Logistics Transp. Rev. 48 (3), 701–714. https://doi.org/10.1016/J.TRE.2011.12.003.

Wang, Z., Silberman, J.A., Corbett, J.J., 2021. Container vessels diversion pattern to trans-Arctic shipping routes and GHG emission abatement potential. Marit. Policy Manag. 1–20. https://doi.org/10.1080/03088839.2020.1795288.

Zhang, Y., Meng, Q., Ng, S.H., 2016. Shipping efficiency comparison between Northern Sea Route and the conventional Asia-Europe shipping route via Suez Canal. J. Transp. Geogr. 57, 241–249. https://doi.org/10.1016/j.jtrangeo.2016.09.008.

Zhang, Q., Wan, Z., Hemmings, B., Abbasov, F., 2019. Reducing black carbon emissions from Arctic shipping: solutions and policy implications. J. Clean. Prod. 241. https://doi.org/10.1016/j.jclepro.2019.118261.

Zhang, Y., Msangi, S., Edmonds, J., Waldhoff, S., 2024. Limited increases in Arctic offshore oil and gas production with climate change and the implications for energy markets. Sci. Rep. 14, 6699. https://doi.org/10.1038/s41598-024-54007-x.